

**Model Study of the Impact of Hydropower Developments on the  
Oceanography of Hudson Bay.**

**by**

**© Ray Roche**

**Submitted to the School of Graduate Studies  
in partial fulfillment of the  
requirements for the degree of  
Master of Science**

**Department of Physics & Physical Oceanography  
Memorial University of Newfoundland**

**June 2017**

**St. John's**

**Newfoundland and Labrador**

## **ABSTRACT**

Hudson Bay is a large inland sea in northern Canada which is characterized by high tides and strong residual currents. It is relatively shallow and isolated from the ocean, and its physical oceanography is largely dependent on freshwater river runoff, surface wind, freshwater and heat fluxes.

The freshwater budget of Hudson Bay has a substantial impact on the environment of the basin, its salinity, stratification of the water column and sea-ice formation. The export of fresh surface waters via the Hudson Strait into the Labrador Sea have been a center of intense studies because of their potential effect on the vertical stratification and deep convection in the Northwest Atlantic Ocean.

Over the past several decades, some of the largest rivers which discharge into Hudson Bay (Nelson, Churchill, Moose, and La Grande Riviere) have been affected by dams, diversions, and reservoirs constructed for generation of hydroelectricity. The thesis presents results from a model study of the impact of this development on the oceanography of Hudson Bay. I use an eddy-permitting, non-tidal model of the North Atlantic and Hudson Bay forced with NCEP atmospheric forcing over the period from 1948 up to 2005. River run-off is determined based on Environment Canada data for 23 rivers which discharge into the HBS collected between 1964 and 2005.

The model results suggest that the hydropower developments in the mid-1970s had two major effects on the characteristics of river runoff into Hudson Bay. Firstly, they reduced the amplitude of seasonal cycle of the freshwater input of some major rivers. Secondly, they caused a change in the spatial distribution of annual mean river runoff. The river diversions had a significant impact on the ocean characteristics of the James Bay. The model simulations suggest that the surface salinity in this region increased since the mid-1970s also affecting processes of vertical mixing and ice-formation.

## ACKNOWLEDGEMENTS

First and foremost, I would like to thank my supervisor, Dr. Entcho Demirov, for his patience and for the many hours he spent sharing his extensive expertise in physical oceanography and computer simulation. Without his invaluable guidance and feedback, this work would not have been possible. I would also like to thank Dr. Joel Heath of the University of British Columbia for suggesting the focus of this research.

I am grateful to my employer, the School of Ocean Technology at the Fisheries and Marine Institute of Memorial University, for the many accommodations allowed in my work schedule which made it possible for me to pursue this educational goal. I am also grateful to Memorial University for the financial assistance provided throughout all my graduate studies in the form of employee tuition support.

I would also like to acknowledge Pat Quigley for perceptive advice many years ago:  
“Keep going out the road [to the schoolhouse] with a pencil behind your ear.”

Last, but certainly not least, I would like to thank my wife and family for their continued support and encouragement throughout this process.

# TABLE OF CONTENTS

Abstract .....	ii
Acknowledgements .....	iii
List of Tables .....	v
List of Figures .....	vi
Chapter 1: Introduction .....	1
1.1 Hudson Bay .....	3
1.2 Climate .....	6
1.3 Water masses and stratification .....	11
1.4 Circulation .....	16
1.5 Research Goals .....	21
Chapter 2: Data and Methods .....	23
2.1 River Discharge Data .....	23
2.2 The Model .....	26
Chapter 3: Decadal variations in the freshwater runoff into Hudson Bay .....	32
3.1 Regulation of river runoff .....	32
3.2 Observed changes in river discharge to Hudson Bay .....	34
Chapter 4: Oceanography of Hudson Bay – model versus observation .....	38
4.1 The Hudson Strait .....	38
4.2 Hudson Bay .....	44
Chapter 5: Impact of river runoff changes .....	51
Chapter 6: Conclusions .....	54
Chapter 7: Future Work .....	56

## LIST OF TABLES

Table 2.1: Annual streamflow statistics .....	25
Table 2.2: Model parameters .....	26

## LIST OF FIGURES

Figure 1.1	Location of Fram, Davis, and Hudson Straits .....	2
Figure 1.2	Hudson Bay watershed.....	4
Figure 1.3	Mean daily air temperature .....	8
Figure 1.4	Freshwater addition by ice cover, runoff (A), precipitation (P), and evaporation (E) for Hudson Bay, using a 1.6 m maximum icecover thickness.....	9
Figure 1.5	Schematic illustration of water masses and the general circulation for Hudson Bay and Foxe Basin.....	13
Figure 1.6	Representative vertical profiles of temperature and salinity in southeastern Hudson Bay at various times of the year .....	15
Figure 1.7	Surface salinities in summer (A) and winter (B) in James Bay .....	15
Figure 1.8	General surface circulation pattern for the summer condition of Hudson Bay and James Bay (Left) (from Prinsenberg, 1986a; numbers are observed velocity values in $\text{cm} \cdot \text{s}^{-1}$ ) compared with surface circulation determined from model results (Right) .....	18
Figure 1.9	Spatial distribution of river tracer during the summer; b) Simulated sea surface salinity for the same period .....	20
Figure 1.10	Mean stress (black Arrows) at the ocean surface for two contrasting periods. Eckman transport (red arrows) is directed towards the right of the stress. The wind stress is taken from the model forcing .....	21
Figure 2.1	Geographical coordinate system ( $\lambda, \phi, z$ ) and the curvilinear coordinate system ( $\mathbf{i}, \mathbf{j}, \mathbf{k}$ ) .....	27
Figure 3.1	Schematic of the evolution of the La Grande River plume from 1976 to 1984 .....	32
Figure 3.2	Comparison of runoff from four of the major rivers most affected by damming or diversion for the pre-1986 and post-1986 periods .....	34
Figure 3.3	Monthly effects of damming on the volume of river runoff .....	35
Figure 3.4	Seasonal effects of damming on the volume of river runoff .....	36
Figure 4.1	Locations of cross-channel (left) and along-channel transects of the study by Drinkwater (1988) .....	39
Figure 4.2	Model simulations (continuous line) and observations (dots) of mean (a) along-channel and (b) across-channel velocity components .....	39
Figure 4.3	Simulated (a) along-channel and (b) cross-channel velocity components averaged over the period 1990-1999 .....	40
Figure 4.4	Observed cross-channel salinity and temperature (upper panels) and simulated salinity and temperature (bottom panels) .....	42

Figure 4.5	Observed (upper panel) and simulated (bottom panel) along-channel salinity and temperature.....	43
Figure 4.6	Location of the salinity profile from St-Laurent et al. (2011).....	44
Figure 4.7	Salinity along 61°N in August 2003 according to (a) model simulation and (b) observations (St. Laurent et al., 2011). Contour interval of the both figures is 0.5 psu.....	45
Figure 4.8	Sea surface (a) salinity and (b) temperature from observations .....	46
Figure 4.9	Simulated (a) surface salinity (psu) and (b) salinity tendency (psu/month) for September – October, 2005 .....	46
Figure 4.10	Simulated (a) sea surface temperature and (b) tendency of sea surface temperature (°C/month) .....	47
Figure 4.11	Comparison of model simulation with sea-ice charts from the Canadian Ice Service for the period of Dec 1996 – August 1997. The first two rows are (a) observed and (b) modeled sea-ice concentration in (%); the last third and fourth rows are (c) observed and (d) modeled sea-ice thickness in cm (0-150) and metres (0-1.5). Note that the data is not available for southern James Bay and are shown as zero values in the observation graphs .....	49
Figure 5.1	Annual mean river flow with averaged SSS (a) and river flow change with salinity difference (b). The location and relative flow of the major rivers are indicated and the change in flow shown as positive (red) or negative (blue) and surface circulation is indicated by the vector plot .....	52
Figure 5.2	Seasonally averaged difference of salinity at 0-20 m (a) and salinity content (kg/m <sup>2</sup> ) in the 20-200m. The averaging periods are, left to right: Jan-Feb-Mar, Apr-May-Jun, Jul-Aug-Sep, and Oct-Nov-Dec.....	53

## **CHAPTER 1. INTRODUCTION**

Heat, salt, and volume fluxes between Arctic and Subarctic and their variations in time have important implications for Global Climate. Bjørn Helland-Hansen and Fridtjof Nansen made the first attempt to quantify these fluxes in 1909. By the late 20th century there was a long observational record, which demonstrated that significant changes were taking place in meridional transport in the ocean with a strong impact on the climates of Arctic and subarctic (Dickson et al., 2008). These observations demonstrated that over the past half century, the waters of the subarctic seas were becoming warmer and ice cover was decreasing. One of the anticipated effects of these changes is modulation of the global Thermohaline Circulation (THC).

The THC, or the global ocean “conveyor”, is responsible for poleward redistribution of heat and salt. A major driver of the THC is deep convection in polar and subpolar ocean where surface cooling causes upper layer waters to sink into the deep part of the ocean (Stewart, 1997). Two of the deep convection areas are located in the Irminger Sea and the Labrador Sea. The freshening of the surface waters of Arctic origin which spread in the Subpolar North Atlantic can potentially affect the density of surface waters exported into the Labrador and Irminger Seas and, hence, to reduce the intensity of deep convection there. Therefore, understanding of the export and spreading of Arctic waters into the subarctic is of crucial importance for understanding dynamics of the Atlantic Meridional Overturning Circulation (AMOC).

The three major conduits for the exchange of freshwater between the Arctic, Sub-arctic seas, and the North Atlantic are the Fram, Davis Straits, and Hudson Bay System. The Fram and Davis straits provide direct links between the Arctic Ocean and the North Atlantic and Nordic Seas. The third pathway for the Arctic waters passes through the Hudson Bay System (HBS) which includes Foxe Basin, Hudson Bay Hudson Strait, and the James Bay (see Figure 1.1). Arctic waters which spread through the HBS are transformed by processes of mixing with the Hudson Bay waters before they enter the Northwest Atlantic. The intense freshwater river discharge in the Hudson Bay additionally contributes to their modification (Straneo and Saucier, 2008). The focus of this thesis is on the impact of the river freshwater runoff on the water mass characteristics of the Hudson Bay.

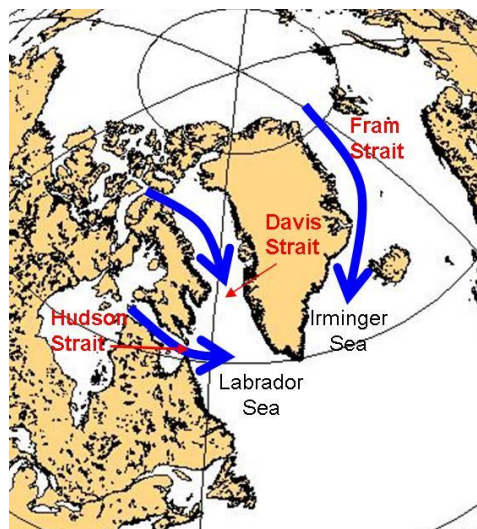


**Figure 1.1.** Location of Fram, Davis, and Hudson Straits

## **Section 1.1 Hudson Bay.**

Hudson Bay is the largest inland sea in northern Canada. The drainage basin of the HBS encompasses an area of 3.7 million square kilometers or more than one third the land mass of Canada, spanning 24° latitude and 47° longitude (Déry et al., 2011). Hudson Bay is bounded in the east by the coast of Quebec, in the south by Ontario and Manitoba, and in the west by Nunavut. The ecosystem receives Arctic marine water from Foxe Basin and freshwater runoff from a catchment basin that is larger than those of the Mackenzie and St. Lawrence rivers combined (Figure 1.2). Precipitation which falls on five Canadian provinces, two territories, and four American states is collected and delivered to the HBS in the form of freshwater river discharge. Hudson Bay spans many different coastal ecozones which offers a broad and varied range of habitats that are used year-round by a range of Arctic and Subarctic biota, and seasonally by many migratory fishes, marine mammals and birds.

There are three key features which characterize the Hudson Bay marine ecosystem:

- extreme southerly penetration of Arctic marine water, which enables polar bear to live and breed in southern James Bay at the same latitude as the holiday resorts in Jasper, Alberta;
- large volume of freshwater runoff that enters it from the land--each year; and
- the dynamic geomorphology of the coastal zone, which is still rebounding from the great weight of the Laurentide Ice Sheet that covered the entire area. New land is emerging from the sea at a rate of up to 15 horizontal m per year along the

stretch of low-lying, marshy coast with its wide tidal flats that continues almost uninterrupted from the Conn River in Quebec to Arviat in Nunavut. (Stewart and Lockhart, 2004)



**Figure 1.2.** Hudson Bay watershed (Stewart and Lockhart, 2004 from Canadian Geographic, 1999).

Precipitation which falls on five Canadian provinces, two territories, and four American states is collected and delivered to the HBS in the form of freshwater river discharge. Long term changes in this freshwater input affect sea-ice formation in the HBS with implication on the climate of northeastern North America (Manak and Mysak, 1989; Weatherly and Walsh, 1996; Saucier et al., 2004). In addition, the freshwater which flows into the HBS is eventually exported via the Hudson Strait into the Labrador Sea, which is one of only three sites in the open ocean where deep water formation takes place. This freshwater influx, by effecting changes to the stratification, is thought to have

a potential impact on the Atlantic meridional overturning circulation (Straneo and Saucier, 2008).

It has also been found that in addition to physical effects on the ocean, there may also be biological consequences for the wildlife in the area. For example, it has been shown that a link exists between ice conditions in Hudson Bay and the breeding patterns of some Arctic-nesting seabirds (Gaston and Hipfner, 1998). Gaston and Hipfner (1998) also suggested that the strong relationships observed between the extent of ice cover and aspects of the breeding biology of the seabirds may reflect conditions affecting the entire marine food web.

In addition to the direct contribution of freshwater flux from the HBS, a significant portion of the Arctic outflow through the Davis Strait is diverted *into* the Hudson Strait and is recirculated through the HBS. The Baffin current, which flows southward through Baffin Bay and the Davis Strait, branches into two currents just north of the mouth of the Hudson Strait at about 63° N. The western branch of this current then flows into the Hudson Strait and is recirculated through the HBS (LeBlond et al., 1981).

The outflow from the Hudson Strait combines with the non-diverted outflow from the Davis Strait and the offshore portion of the West Greenland current into the Labrador Current. This current flows close to one of the regions of deep convection in the Labrador Sea (Straneo and Saucier, 2008). After the turbulent mixing during the deep convection period of the winter months, the highly stratified and relatively fresh Labrador Current helps re-stratify this region in the spring (Straneo, 2006).

Over the surface of James Bay only, where precipitation is much greater than evaporation and runoff is high, there is an annual net gain of 473 cm of fresh water (Figure 1.4). This is much greater than the combined average for Hudson/James Bay, where Hudson Bay loses more fresh water through evaporation than it gains from precipitation, and there is an annual net gain of only 64 cm over the entire marine surface. Consequently, runoff has a strong influence on oceanographic and ice conditions, particularly in James Bay.

Temperature and precipitation vary widely in time and space over this region, with precipitation ranging from less than 200 mm per year in the northwest to over 800 mm per year in the southeast (Stewart and Lockhart, 2004).

The goal of this thesis is to study the impact of this river discharge variation on the oceanography and climate of Hudson Bay. The following sections provide background information on the climate and oceanography of Hudson Bay.

## **Section 1.2 Climate**

Hudson Bay climate is abnormally cold relative to other areas at the same latitude, with long and cold winters and cool summers. It also differs from north to south and east to west. The harshest climate is found in northwestern Hudson Bay where there is the greatest influence of cold Arctic air masses and it is the coldest part of Canada based on wind chill (Figure 1.3). Other areas have either moderating southern or marine influences. Hudson Bay is fully ice-covered in winter and ice-free in August and

September. Since the links of the HBS with the open ocean is limited, the cycles of sea ice cover are believed to be dominated by the atmospheric forcing (Wang et al., 1994b).

Ice cover plays a central role in surface heat budget of Hudson Bay in two major aspects:

- 1) the ice cover has a high albedo and thereby decreases the amount of short wave insolation which is absorbed by the surface; and
- 2) ice acts as an insulator between the ocean water and the colder atmosphere, which decreases the amount of heat loss to the atmosphere.

Winter net heat flux in Hudson Bay is small and is dominated by surface loss due to long wave radiation. (Danielson, 1969). In spring (April – May), incoming shortwave solar radiation increases sharply. Initially this increase is balanced by the intense surface turbulent heat loss. With the time, however, the surface heat loss is reduced to near zero as the surface temperature approaches the melting point.

The summer heat budget, from May through August, is dominated by shortwave insolation. Turbulent heat loss is reduced because the near surface air is hydrostatically stable. Net heat influx during this period is enough to completely melt all the ice cover (Danielson, 1969). In September, insolation decreases and long wave and turbulent heat losses dominate. By January the bay is completely ice-covered again. Heat loss continues throughout the winter resulting in a maximum ice thickness in April.

Over an annual cycle, the radiative and turbulent terms of the heat budget of Hudson Bay result in a slight surplus of heat intake. This surplus is balanced by the advective term in the heat budget which represents heat carried away by currents. Geographically, the greatest heat gain occurs in the western part of the bay while the eastern part is dominated by heat loss (Danielson, 1969).

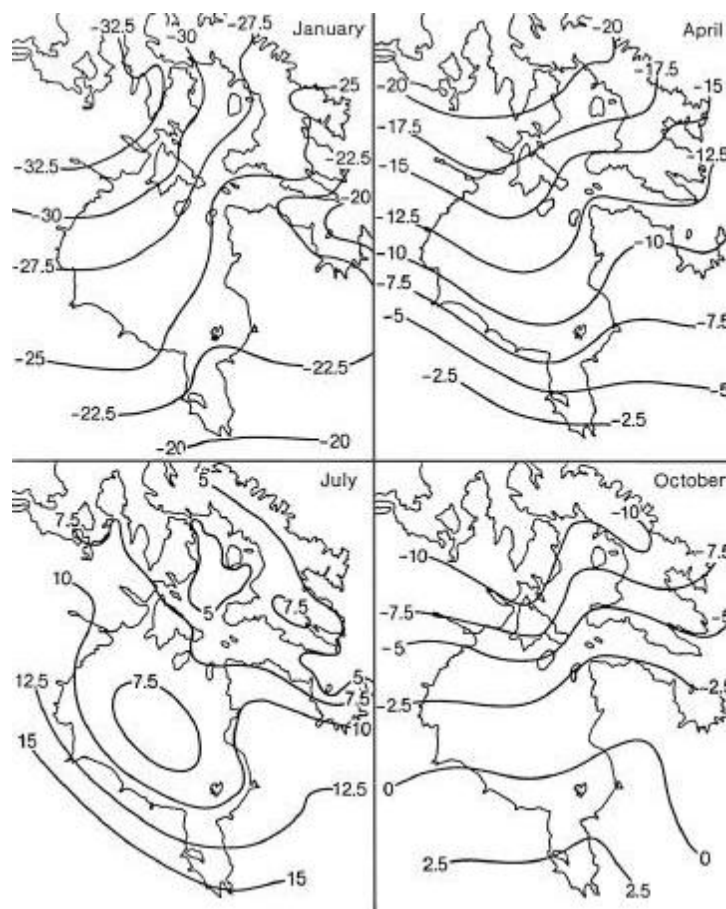


**Figure 1.3.** Mean daily air temperature (°C) (from Maxwell, 1986).

In James Bay runoff is high, there is an annual net gain of 473 cm of fresh water over the entire surface. This is much greater than the average for Hudson/James Bay,

where more fresh water is lost through evaporation than is gained from precipitation and has an annual net gain of only 64 cm over the entire marine surface (Stewart & Lockhart, 2004). Consequently, runoff has a strong influence on oceanographic and ice conditions, particularly in James Bay.

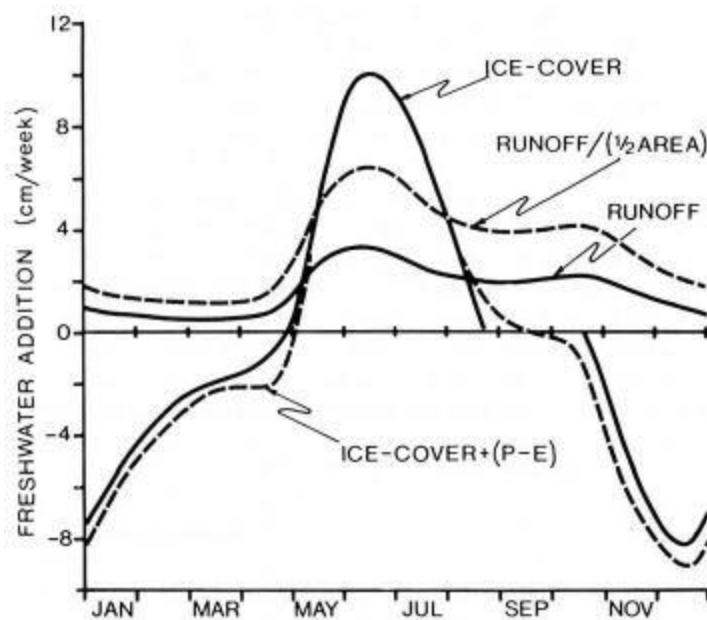


**Figure 1.4.** Freshwater addition by ice cover, runoff (A), precipitation (P), and evaporation (E) for Hudson Bay, using a 1.6 m maximum icecover thickness (adapted from Prinsenberg, 1988b)

The climate of Hudson Bay has a strong influence on the surrounding land area, contributing particularly to the unusual southern extent of the permafrost. Permafrost is soil, rock or sediment that is frozen for more than two consecutive years. In areas not overlain by ice, it exists beneath an "active layer" layer of soil, rock or sediment, which freezes and thaws annually.

Spatial variations in the Hudson Bay climate characteristics determines the presence of four ecozones along the coastlines of Hudson and James Bays. These four Terrestrial Ecozones are: 1) Hudson Plains, 2) Taiga Shield, 3) Southern Arctic, and 4) Northern Arctic (Marshall and Schut, 1999). These regions are not delineated based on climatic data, rather on their responses to climate as expressed by vegetation and reflected in soils, wild life, and water. Moving from south (Hudson Plains) to north (Northern Arctic) trends are apparent in the vegetation, which changes from boreal forest to tundra. The southward deflection of these broad east-west ecozones in the Hudson Bay-James Bay emphasizes the magnitude of the climatic effect of the extreme southerly penetration of Arctic waters in this marine ecosystem. (Stewart and Lockhart, 2004).

The normal sea-ice cycle in Hudson Bay is that it is nearly completely ice-covered from November to June and ice free during the summer months. Hudson Bay is ice-free from September through November, while Foxe Basin is normally only ice-free during September, (Prinsenberg, 1986a). The maximum sea-ice thickness varies from a high of more than 2 m in the north of Foxe Basin to a low of less than 1.5 m in southern Hudson Bay and eastern Hudson Strait (Prinsenberg, 1988)

Interannual sea-ice anomalies in Hudson Bay are found to be related to the North Atlantic Oscillation (NAO) and the Southern Oscillation (SO) as found by Wang et al. (1994b). The existence of decadal-scale fluctuations in ice cover in the Labrador Sea was first noted by Manak and Mysak (1989). They suggested that these fluctuations could be due to decadal-scale sea surface temperature anomalies in the northwest North Atlantic,

or to the 7-8 year periodicity in the NAO. The possible influence of Pacific atmospheric circulation anomalies on Hudson Bay-Labrador Sea ice cover could be inferred from another study published by Van Loan and Madden (1981) which showed that certain Northern Hemisphere interannual variations in sea-level pressure (SLP) and air temperature were associated with the SO in the tropical Pacific.

Sea-ice cover in Hudson Bay responds to a Low/Wet episode of the SO (defined as the period when the SO index becomes negative) mainly in summer, when the sea-ice cover has a large positive anomaly that starts in summer and continues through to autumn. The sea-ice cover anomalies in the region respond to the SO and SAT on the approximate time scales of 1.7-year, 5-year and 10-year periods. Sea ice has a positive anomaly during the strong westerly NAO events. (Wang et al., 1994b)

### **Section 1.3 Water Masses and Stratification**

Three major types of water masses with different characteristics enter the Hudson Bay System: river runoff, Arctic Ocean waters which enter Foxe Basin through the Fury and Hecla Straits and Labrador Sea waters inflow through the Hudson Strait.

The annual runoff to Hudson Bay corresponds to a freshwater layer of 0.78 m, if averaged over the entire surface area of the bay (Prinsenbergh, 1988). The large volume of the runoff enters James Bay and has a great effect on the oceanography of this region. The timing and pattern of the breakup of ice cover, the surface circulation, water column

stability, species distributions, and biological productivity are influenced by this freshwater input.

In spring and summer, the cold saline Arctic surface water that enters Hudson Bay and mixes with meltwater and runoff from the land. These surface waters are warmed by the sun, and mixed by the wind as they circulate through Hudson Bay and James Bay. The resulting strengthening of vertical stratification influences the ecosystem in summer through slowing of vertical mixing. In winter, this stratification is weakened by lower runoff and surface layer cooling and mixing.

The third type of water which enters the Hudson Bay System through the mouth of Hudson Strait is a mixture of Baffin Bay and Labrador Sea waters. This so called the Hudson Strait Bottom Water which flows westward while mixing with overlying water. The mixing of these three water types, along with sea-ice production and melting, produce a range of water masses (Jones and Anderson, 1994). The main water masses of Hudson Bay are shown schematically in Figure 1.5 along a north-south transect from Fury and Hecla strait in the north, through Southampton Island, to Hudson Bay in the south.

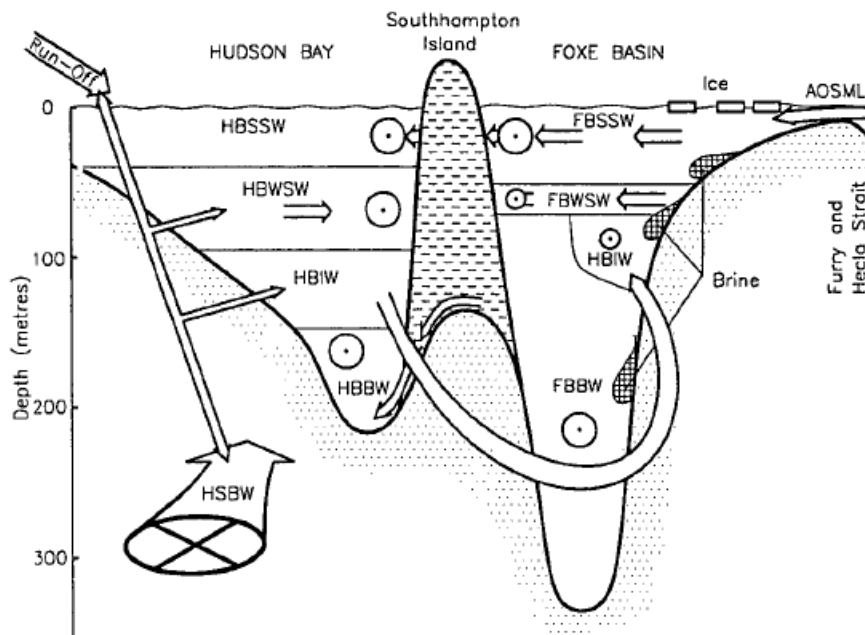


**Figure 1.5.** Schematic illustration of water masses and the general circulation for Hudson Bay and Foxe Basin. (Jones and Anderson, 1994 p372)

Nine water masses are identified in the figure are as follows:

AOSML	Arctic Ocean Surface Mixed Layer
FBBW	Foxe Basin Bottom Water
FBSSW	Foxe Basin Summer Surface Water
FBWSW	Foxe Basin Winter Surface Water
HBBW	Hudson Bay Bottom Water
HBIW	Hudson Bay Intermediate Water
HBSSW	Hudson Bay Summer Surface Water
HBWSW	Hudson Bay Winter Surface Water
HSBW	Hudson Strait Bottom Water

Inside Hudson Bay, Hudson Strait Bottom Water mixes with surface layer waters and forms both Hudson Bay Winter Surface Water and Hudson Bay Intermediate Water. Hudson Bay Winter Surface Water then mixes with sea-ice meltwater to form Hudson Bay Summer Surface Water (Jones and Anderson, 1994).

The waters in Foxe Basin, while marginally affected by the inflow from Hudson Strait, are affected to a much greater degree by water of the Arctic Ocean Mixed Surface Layer coming from the Arctic Ocean into Foxe Basin through Fury and Hecla Strait (Jones and Anderson, 1994). Some Hudson Bay Intermediate Water enters the southeastern part of Foxe Basin at a depth of about 100 m, but this water does not seem to penetrate very far into the Basin.

Foxe Basin Bottom Water overflows into Hudson Bay and mixes with Hudson Bay Bottom Water. The salinity of Foxe Basin Bottom Water is significantly higher than that of either the Arctic Ocean Surface Mixed Layer or the Hudson Strait Bottom Water. (Jones and Anderson, 1994). According to Prinsenber (1986a), the most likely source of salt for this high salinity in Foxe Basin is brine released during the production and aging of sea ice.

The vertical stratification in Hudson Bay is relatively stable below 50 m depth, (Figure 1.6) where the water becomes progressively colder and more saline with depth. At about 100 m, the mean temperature is less than  $-1.4^{\circ}\text{C}$  and salinity greater than 33 ppt. The deep water layer in James Bay is subject to considerable seasonal and interannual variation in temperature and salinity, due in part to the relative shallowness of the bay.

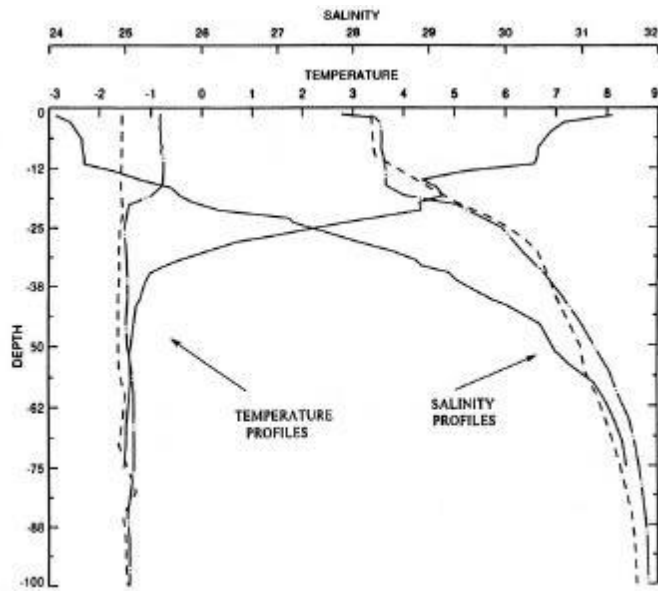


**Figure 1.6.** Representative vertical profiles of temperature and salinity in southeastern Hudson Bay at various times of the year (different years); April 15, 1982 (dashed line), May 16, 1982 (dashed-dotted line), August 15, 1976 (solid line) (from Ingram and Prinsenber, 1998:851).

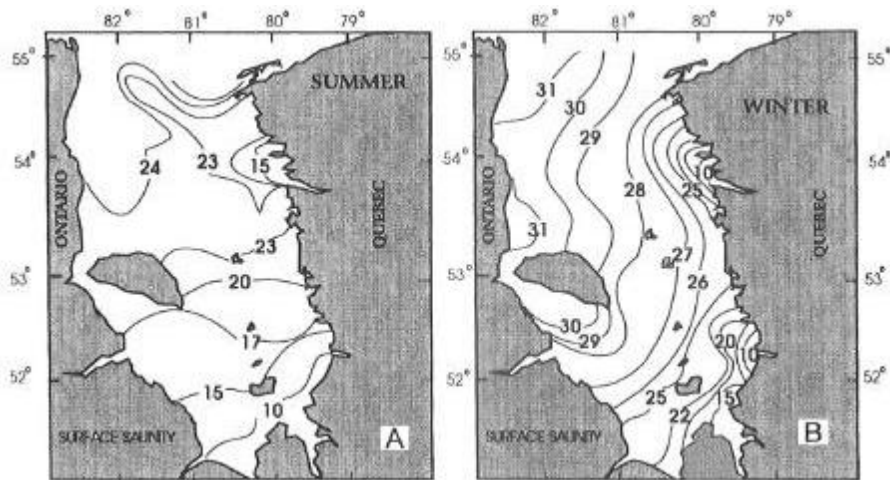


**Figure 1.7.** Surface salinities in summer (A) and winter (B) in James Bay (adapted from Ingram and Prinsenber, 1998).

Subsequent to hydroelectric developments, extensive freshwater plumes are observed off the river mouths in James Bay (Figure 1.7) year round. In winter, these plumes spread further and deeper under the ice despite runoff rates that are an order of magnitude lower than in summer. These effects are most pronounced in eastern James Bay and along the southeastern coast of Hudson Bay. Freshwater runoff affects the primary productivity both positively and negatively: negatively by increasing vertical stability of the water column, and positively through nutrient additions--either direct or due to deep-water entrainment (Stewart and Lockhart, 2004).

## Section 1.4 Circulation

Hudson Bay is relatively shallow and relatively isolated from the ocean; as a result its physical oceanography is largely dependent on freshwater river runoff, local wind stress, radiation heat flux and annual ice cover. Experiments using bottle drift, salinity and temperature data show that the summer circulation of the Hudson Bay and James Bay is cyclonic (Prinsenber, 1986b).

The baroclinic radius of deformation is given by:

$$R_d = \frac{\sqrt{g'h}}{f}$$

where:

$g' = g \frac{\rho_d - \rho_s}{\rho_0}$  is the reduced gravity,  $h$  is the depth and  $f$  is the Coriolis parameter.

With typical values for Hudson Bay of:

$$g' = 0.01 \text{ m} \cdot \text{s}^{-2}, \quad h = 200 \text{ m}, \quad f = 1.3 \times 10^{-4}$$

Which gives:

$$R_d = \frac{\sqrt{g'h}}{f} = \frac{\sqrt{(0.01 \text{ m} \cdot \text{s}^{-2})(200\text{m})}}{1.3 \times 10^{-4} \text{ s}^{-1}} = \frac{\sqrt{2}}{1.3 \times 10^{-4} \text{ s}^{-1}} \frac{\text{m}}{\text{s}} \approx 1 \times 10^{-4} \text{ m} = 10 \text{ km}$$

This value corresponds well with the range of 7 – 10 km for the Rossby radius of deformation defined by Straneo & Saucier (2008)

The driving factors of the circulation are the predominant cyclonic direction of the wind and the water mass flux in and out of the region. A major influx occurs along the west coast of Southampton Island which consists mostly of salty and dense Atlantic waters; these waters sink and spread southward into Hudson Bay. Another important inflow is the freshwater from rivers flowing into James Bay which spreads along the east coast of Hudson Bay. These two major streams shape the general cyclonic circulation of Hudson Bay.

The observed summer circulation as shown in Figure 1.8, exhibits a southeastward flow along the southern shore with a velocity of 5.0 cm/s. The flow along the eastern coast of Hudson Bay has a northwestward direction. The waters transported by these currents interact and mix in a complex way. The waters which enter from Hudson Strait and Foxe Basin are denser and sink to depths of 200 m. The waters transported along the east coast are relatively fresh and spread in the surface layer.

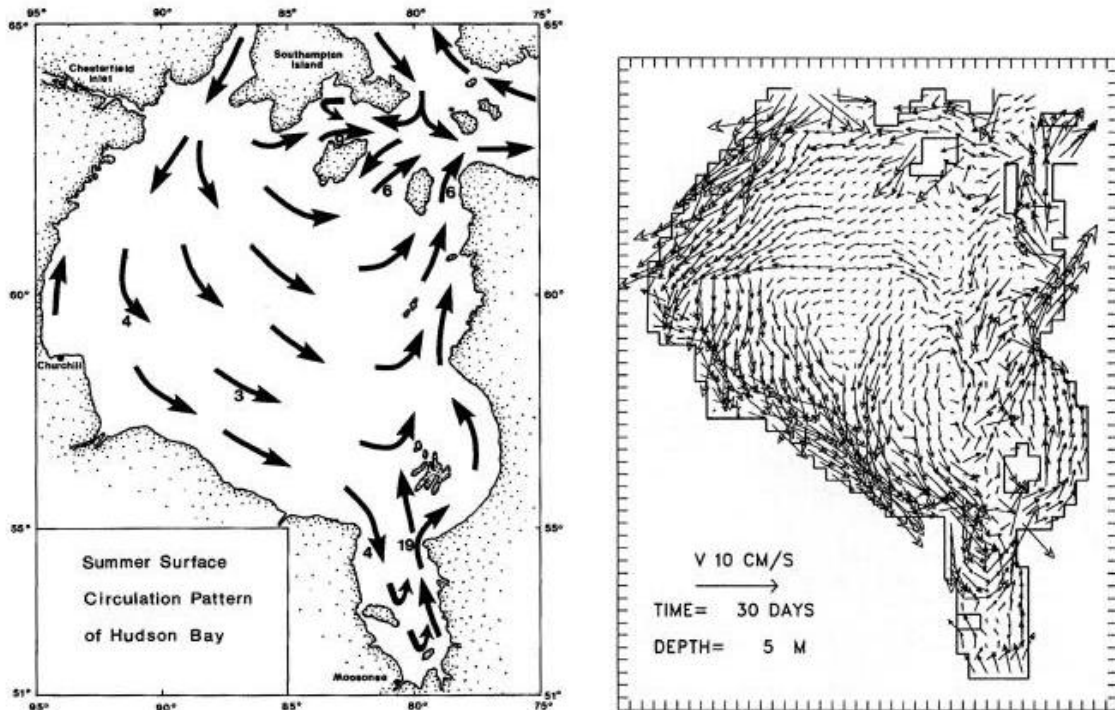


**Figure 1.8.** General surface circulation pattern for the summer condition of Hudson Bay and James Bay (Left) (from Prinsenberg, 1986a; numbers are observed velocity values in  $\text{cm} \cdot \text{s}^{-1}$ ) compared with surface circulation determined from model results (Right) (from Ingram and Prinsenberg, 1996 as modified by J. Wang from Wang, 1993).

Winter circulation is poorly known. Available observations are limited to that obtained from one year long current meter mooring stations located 150 km northeast of Churchill, Manitoba. (Prinsenberg and Weaver, 1983).

The observed hourly averaged currents in Hudson Bay are dominated by semi-diurnal tidal components, while the daily averaged currents are dominated by components with five and six day periods and are wind-generated, inertial currents caused by passing weather systems. The year-long mooring data indicates that the circulation pattern varies

with the season and the tidal components are reduced by 20% during the ice-covered period due to friction. (Prinsenber,1986b)

A model study of St. Laurent et al. (2011), simulated the spreading of passive tracers injected at the same of locations as the outflow from some main rivers. The highest concentrations are found near the shorelines, and most river plumes are deflected toward the right as expected from the Coriolis force. The tracer field evolves over time by moving in a counter-clockwise sense and leaving partly through Hudson Strait, which is consistent with the known currents of the basin (Prinsenber, 1986a). What is less expected is that the river waters seem to be only loosely trapped to the coastlines, leaking toward the interior of the basin at scales of 100 km rather than 10 km.

The existence of such seaward transport is supported by a certain number of observations (Granskog et al., 2009). Figure 1.9 shows the simulated surface salinity (Figure 1.9a) and the tracer concentration from (Figure 1.9b). These simulations suggest that there is a significant cross-shore transport which partly diverts the river waters from their spreading towards the Hudson Strait.

Two processes are likely to contribute to the cross-shore transport of freshwater: 1) Ekman transport due to dominant wind field (Figure 1.10) in the surface layer (e.g., Lentz, 2004); and 2) eddies formed through baroclinic instability of the boundary current (e.g., Spall, 2004).

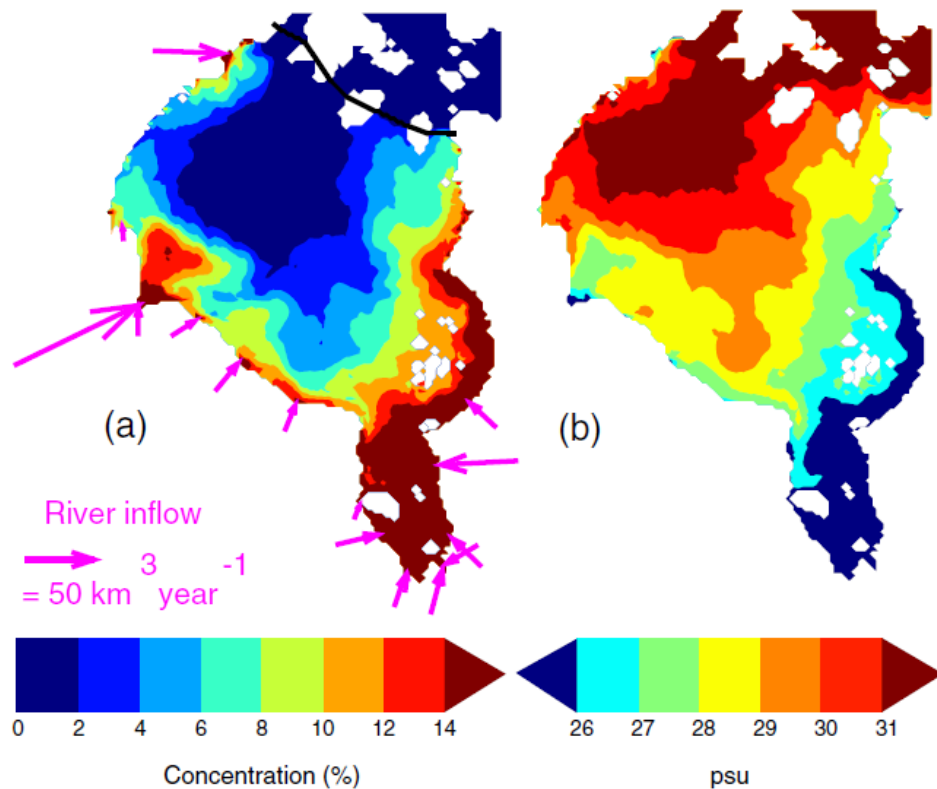


**Figure 1.9.** Spatial distribution of river tracer during the summer; b) Simulated sea surface salinity for the same period (St. Laurent et al., 2011).

The impact of the surface wind is not fully understood. Hudson Bay is ice free for 2-3 months per year and is completely ice covered for 2-3 months in the winter. During the rest of the year Hudson Bay is partly ice free. The wind driven currents are generated during the time of the year when Hudson Bay is ice free or partly ice covered. In particular, it is observed that wind driven phenomena like coastal upwelling can be especially strong in the late spring.

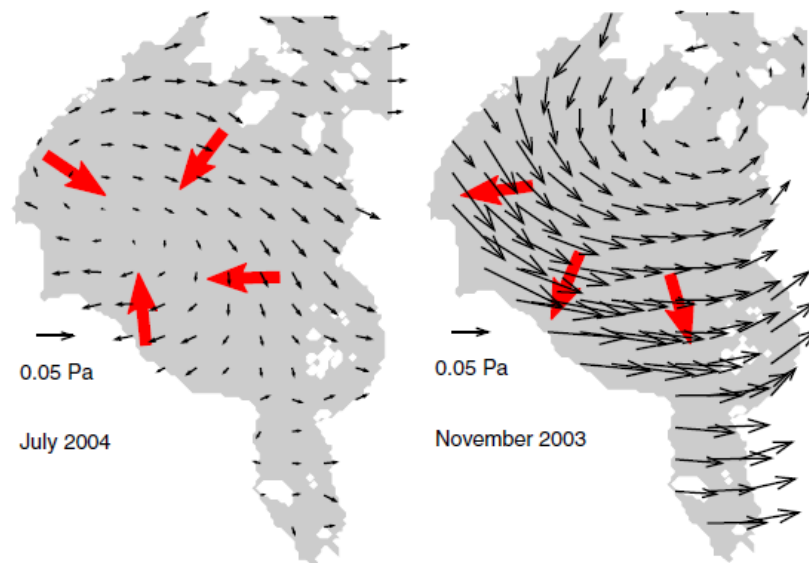


**Figure 1.10** Mean stress (black Arrows) at the ocean surface for two contrasting periods. Eckman transport (red arrows) is directed towards the right of the stress. The wind stress is taken from the model forcing (St-Laurent et al., 2011)

The study by St-Laurent et al. (2011), finds that the transit time is three years for fresh water to exit the bay; however their results also show that about 25% of the fresh water is diverted into the interior of the basin and it is estimated that this diversion accounts for an increase of about 0.8 years in the total transit time.

## Section 1.5 Research Goals

The aim of this study is to use a numerical ocean model to investigate the possible effects of variability in freshwater runoff to the Hudson Bay System. This investigation will be carried out by modeling the results of imposing a “flattening” on the seasonality

regime of the total annual runoff. The intent is to evaluate the effect of these changes on properties such as surface salinity and ice cover.

Two model simulations were used, each using a different regime of freshwater runoff data. The first simulation used actual river runoff data from 1964 to 1999. The second simulation used actual river runoff from 1964 to 1986, the year of the first major hydroelectric project in Hudson Bay. From 1986 to 1999, the monthly mean runoff based on pre 1986 data was used; the intent being to simulate what would have happened if the hydroelectric developments had not occurred. Comparison of the output data from both simulations provides a representation the impact of the hydroelectric development in Hudson Bay.

Specifically of interest will be the identification of any potential changes in the circulation patterns and in timing and duration of sea-ice formation. These are factors which can impact wildlife within Hudson Bay and potentially affect the freshwater transport from Hudson Bay into the Labrador Sea.

We are considering that the interaction between the Hudson Bay system and the Labrador Sea is a major factor that influences the response of the Hudson Bay system to the variations in the river discharge.

## **CHAPTER 2. DATA AND METHODS**

In this study we use an ocean general circulation *model Nucleus for European Models of the Ocean* (NEMO) (Madec, 2008) to study the circulation in Hudson Bay. The model domain includes North Atlantic and the Hudson Bay System. The ocean model is forced surface momentum and buoyancy fluxes, lateral transport from the Arctic, and river input for the period of time from 1950 to 2005. A major focus of this study is on the impact which anthropogenically driven variations of river input have on the oceanography characteristics of the basin.

### **Section 2.1 River Discharge Data**

Over the past several decades, some of the largest of all the rivers which discharge into the HBS (Nelson, Churchill, Moose, and La Grande Riviere) have been affected by dams, diversions, and reservoirs constructed for generation of hydroelectricity. The first phase of the James Bay Hydroelectric complex in Quebec involved the construction of several large reservoirs on La Grande Riviere between 1979 and 1986 (Déry and Wood, 2004). 1986 is therefore used as the pivotal year, which divides the overall study period into the pre-development and post-development phases. The model experiments and data analysis were correspondingly designed to examine the study parameters before and after 1986.

The study uses data collected over a 45 year period from 1964 up to 1999. Discharge data for 23 rivers (see Table 2.1) which discharge into the HBS was obtained from *Environment Canada's* HYDAT hydrometric database for this time period. This is data captured at streamflow stations at the mouth of each of the 23 rivers and contains the daily and monthly means. This database can be downloaded from *Environment Canada's* website at [<https://ec.gc.ca/rhc-wsc/default.asp?lang=En&n=9018B5EC-1>].

Matlab was used to reconfigure the datasets to comply with the *NETwork Common Data Format* (NetCDF) specification. These NetCDF files were then used as input to the model to provide surface freshwater flux data. The source data was provided in units of  $\text{km}^3$  per month and was converted to units of  $\text{m}^3$  per second.

Results from two model experiments are used in this thesis to assess the effects of the anthropogenically driven change of the river runoff on the oceanography of Hudson Bay. The two experiments were configured to encompass the three decade period from 1970 until 1999, inclusive. This period was chosen to balance about the year 1986, which was the year when the first significant hydro-electric development project in Hudson Bay became active.

**EXP 01** – The model river discharge forcing was the actual river discharge for all years of simulations (1950 - 1999).

**EXP 02** – The river forcing was calculated based in data from the pre-damn period. The river data from the period before 1985 were used to calculate monthly mean

river discharge. This forcing was to run the model initialized with the simulations from EXP01 starting from 1985.

The results of the EXP01 and EXP02 are compared for the period from 1990 to 1999.

**Table 2.1: Annual Streamflow Statistics**

River	Mean (km <sup>3</sup> )
<b>Manitoba</b>	
Churchill	19.4
Hayes	19.4
Nelson	92.6
Seal	11.4
<b>Nunavut Territory</b>	
Chesterfield Inlet	41.3
Thlewiaza	6.9
<b>Ontario</b>	
Albany	31.9
Attawapiskat	11.7
Ekwan	2.7
Moose	39.7
Severn	21.3
Winisk	15.2
<b>Quebec</b>	
Boutin	0.5
Broadback	10.0
Eastmain	12.8
Grande Rivière de la Baleine	19.6
Harricana	10.9
La Grande Rivière	80.5
Nastapoca (Loups Marins)	8.0
Nottaway	31.4
Petite Rivière à la Baleine	3.7
Pontax	3.1
Rupert	26.7
<b>All Rivers</b>	<b>520.7</b>

## Section 2.2 The Model

NEMO, the numerical model used in this study, is a primitive equation, free surface ocean circulation model OPA9 (Madec, 2008) coupled with the multi-layered sea ice code LIM2 (Fichefet and Morales Maqueda, 1997). The model parameters are summarized in Table 2.2.

Table 2.2. Model Parameters	
Name of model	NEMO
Horizontal resolution	$0.25^\circ \times 0.25^\circ \cos \phi$
Horizontal dimensions	$544 \times 336$
Time step (s)	2,400
Max horizontal resolution (km)	27.6
Min horizontal resolution (km)	11.0
Max biharmonic viscosity ( $\text{m}^4/\text{s}$ )	$1.5\text{E}+11$
Max Laplacian diffusivity ( $\text{m}^2/\text{s}$ )	300

### Governing equations

The equations of the NEMO are the incompressible Boussinesq, thin-shell, hydrostatic primitive equations of ocean fluid mechanics. They include the equations of conservation of momentum, mass, and heat for the ocean written in general orthogonal curvilinear coordinates. In this study we use the NEMO code implemented in vector-invariant form:

$$\frac{\partial \mathbf{U}_h}{\partial t} = - \left[ (\nabla \times \mathbf{U}) \times \mathbf{U} + \frac{1}{2} \nabla (\mathbf{U}^2) \right]_h - f \mathbf{k} \times \mathbf{U}_h - \frac{1}{\rho_0} \nabla_{hP} + \mathbf{D}^U + \mathbf{F}^U \quad (2.1a)$$

$$\frac{\partial p}{\partial z} = -\rho g \quad (2.1b)$$

$$\nabla \cdot \mathbf{U} = 0 \quad (2.1c)$$

$$\frac{\partial T}{\partial t} = -\nabla \cdot (T \mathbf{U}) + D^T + F^T \quad (2.1d)$$

$$\frac{\partial S}{\partial t} = -\nabla \cdot (S \mathbf{U}) + D^S + F^S \quad (2.1e)$$

$$\rho = \rho(T, S, p) \quad (2.1f)$$

Where:  $g$  = acceleration due to gravity  
 $\mathbf{U}$  = horizontal velocity  
 $T$  = temperature  
 $S$  = salinity  
 $\rho$  = density

These equations are written in spherical coordinates  $(\lambda, \phi, z)$  defined by the latitude  $\phi$ , the longitude  $\lambda$  and the distance from the centre of the earth  $a+z(k)$  where  $a$  is the earth's radius and  $z$  the altitude above a reference sea level (Fig.2.1).

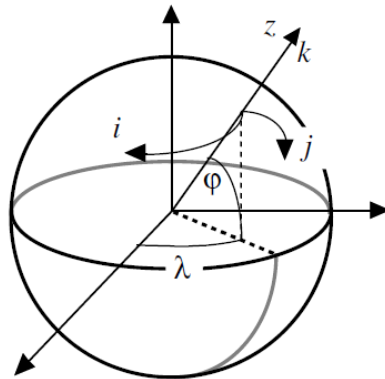


**Figure 2.1** Geographical coordinate system  $(\lambda, \phi, z)$  and the curvilinear coordinate system  $(i, j, k)$

The local deformation of the curvilinear coordinate system is given by metric factors  $e_1$ ,  $e_2$  and  $e_3$ :

$$\begin{aligned} e_1 &= (a+z) \left[ \left( \frac{\partial \lambda}{\partial i} \cos \varphi \right)^2 + \left( \frac{\partial \varphi}{\partial i} \right)^2 \right]^{1/2} \\ e_2 &= (a+z) \left[ \left( \frac{\partial \lambda}{\partial j} \cos \varphi \right)^2 + \left( \frac{\partial \varphi}{\partial j} \right)^2 \right]^{1/2} \\ e_3 &= \frac{\partial z}{\partial k} \end{aligned} \quad (2.2)$$

The thin-shell approximation is used which is based on assumption that ocean depth is far smaller than the earth's radius. Therefore,  $a+z$  in equations (2.2) is replaced by  $a$ . The resulting horizontal scale factors  $e_1, e_2$  are independent of  $z$  while the vertical scale factor is a function of vertical index  $k$ . In these notations, the scalar and vector operators that appear in the primitive equations (Eqs. (2.1a) to (2.1f)) are written in the tensorial form in general orthogonal horizontal curvilinear coordinate system:

$$\nabla q = \frac{1}{e_1} \frac{\partial q}{\partial i} \mathbf{i} + \frac{1}{e_2} \frac{\partial q}{\partial j} \mathbf{j} + \frac{1}{e_3} \frac{\partial q}{\partial k} \mathbf{k} \quad (2.3a)$$

$$\nabla \cdot \mathbf{A} = \frac{1}{e_1 e_2} \left[ \frac{\partial (e_2 a_1)}{\partial i} + \frac{\partial (e_1 a_2)}{\partial j} \right] + \frac{1}{e_3} \left[ \frac{\partial a_3}{\partial k} \right] \quad (2.3b)$$

$$\begin{aligned} \nabla \times \mathbf{A} &= \left[ \frac{1}{e_2} \frac{\partial a_3}{\partial j} - \frac{1}{e_3} \frac{\partial a_2}{\partial k} \right] \mathbf{i} + \left[ \frac{1}{e_3} \frac{\partial a_1}{\partial k} - \frac{1}{e_1} \frac{\partial a_3}{\partial i} \right] \mathbf{j} \\ &\quad + \frac{1}{e_1 e_2} \left[ \frac{\partial (e_2 a_2)}{\partial i} - \frac{\partial (e_1 a_1)}{\partial j} \right] \mathbf{k} \end{aligned} \quad (2.3c)$$

$$\Delta q = \nabla \cdot (\nabla q) \quad (2.3d)$$

$$\Delta \mathbf{A} = \nabla (\nabla \cdot \mathbf{A}) - \nabla \times (\nabla \times \mathbf{A}) \quad (2.3e)$$

where  $q$  is a scalar quantity and  $\mathbf{A} = (a_1, a_2, a_3)$  a vector in the (i, j, k) coordinate system (Figure 2.1).

### **Model configuration**

As discussed in the introduction, the Hudson Bay System is part of one of the major conduits connecting the Arctic and the North Atlantic. Some previous studies (Saucier 2004, St. Laurent 20112) simulated the Hudson Bay dynamics by defining boundary conditions at the east end of the Hudson Strait. Those studies provide reasonable results when performing simulations for a few years. This study is focused on multi-decadal variations in the Hudson Bay system in response to the variation in river discharge. Therefore, considering the fact that the Hudson Bay system is part of one of the major conduits between the Arctic and the North Atlantic, our model design considers the feedbacks which exist between the circulation of the North Atlantic and the Hudson Bay system. In Hudson Bay, the model grid has horizontal resolution of about 12 km and 24 vertical levels.

The model domain covers the North Atlantic from  $7^\circ$  N to  $67^\circ$  N with a Mercator isotropic longitude  $\times$  latitude grid and 46 vertical levels. The horizontal resolution is  $1/4^\circ$  in longitude and  $1/4^\circ \cos \phi$  in latitude. This resolution corresponds to model grid spacing of 11-12 km in the Hudson Bay System. A free-slip boundary condition is applied at land boundaries. Open boundary conditions (OBC) at the northern and southern boundaries are defined according to the formulation by Tréguier et al. (2001) and Marchesiello et al.

(2001). These are radiation OBC which constrain the long-term variability of model quantities at the open boundaries by their climatological values, which in the present study are defined from SODA data (Carton et al., 2005). Vertical grid spacing is irregular with 8 m resolution at the surface, which smoothly increases to 280 m at 5,600 m.

The model bathymetry is derived from the 2-min resolution ETOPO2 bathymetry file of National Geophysical Data Center (US Department of Commerce et al., 2006). The bathymetry data are interpolated on the model grid by using the median method, and then two passes of Shapiro filter is applied to the topography. A few hand edits are performed, such as removing some closed seas.

Partial step (Adcroft et al., 1997) method is applied to represent topography. The energy–enstrophy conserving scheme (Arakawa and Lamb, 1981), which conserves total energy for general flow and potential enstrophy for flows with no mass flux divergence, is used in momentum equations. These options were found to get the better performance in the simulations of the North Atlantic by the previous studies of Barnier et al. (2006) and Penduff et al. (2007).

The vertical mixing is parameterized by the 1.5 turbulent closure model of Gaspar et al. (1990), adapted to OPA by Blanke and Delecluse (1993). In case of static instability, a viscosity /diffusivity enhancement of  $10 \text{ m}^2/\text{s}$  is used. A Laplacian lateral isopycnal diffusion on tracers is used ( $300 \text{ m}^2/\text{s}$  at  $7^\circ \text{ N}$  and decreasing poleward proportionally to the grid size), while a horizontal biharmonic viscosity is used for

momentum ( $-1.5 \times 10^{11}$  m<sup>4</sup>/s at 7° N and decreasing poleward as the cube of the grid size).

Near the coast, there is a strong current of freshwater originating from rivers. This current, which is directed along the density front separating the the river water mass from the interior, is potentially unstable as it is subject to baroclinic instability, meandering, and eddy formation. The mesoscale and submesoscale constitute potentially important processes of cross-shore exchange. These are not resolved by this model since it is not an eddy resolving model. Instead they are parameterized by isopycnal diffusion and following a standard approach used in climate models. (Gent and McWilliams, 1990).

Initial conditions for temperature and salinity are derived from WOA05 dataset (Locarnini et al. 2006; Antonov et al. 2006) for the North Atlantic and Baltic Sea and from MEDAR dataset (Brankart and Brasseur, 1998) for the Mediterranean Sea. The model is forced by surface heat, freshwater, and momentum fluxes which are computed with climatological monthly mean. The latter are derived from the NCEP/NCAR reanalysis (Kalnay et al., 1996) for the period of time from 1968 to 1996.

## CHAPTER 3. DECADAL VARIATIONS IN THE FRESHWATER RUNOFF INTO HUDSON BAY

### 3.1 Regulation of river runoff

The Hudson Bay system receives freshwater runoff from a catchment basin that is larger than those of the Mackenzie and St. Lawrence rivers combined (Figure 1.2). It is therefore reasonable to assume that significant changes in the seasonality of this runoff may have an effect on this ecosystem. Hydro-electric developments have altered the flow regimes of the La Grande and Eastmain rivers, which drain into James Bay, and of the Churchill and Nelson rivers, which drain into southwest Hudson Bay.

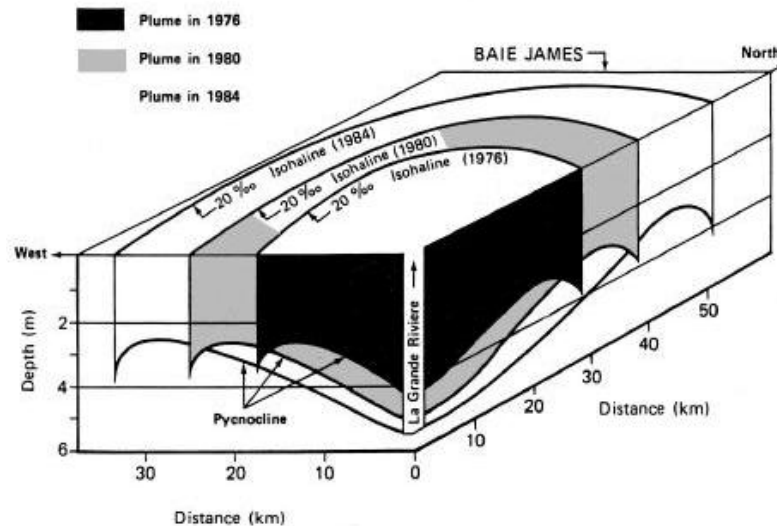


**Figure 3.1.** Schematic of the evolution of the La Grande River plume from 1976 to 1984 (from Messier et al. 1986).

In 1980, 80% of the flow from the Eastmain River was diverted into the La Grande River, and seasonal runoff was impounded so that it could be released to produce electricity in the winter; consequently, the natural spring freshet into James Bay does not occur at either river. The plume from the Eastmain River is now much smaller and the size and shape of the summer plume from the La Grande River are essentially unchanged; however, the area of the under-ice plume from the La Grande River has trebled (Figure 3.1) and can now extend 100 km northward under the landfast ice of James Bay.

75% of the flow of from the Churchill River has been diverted into the Nelson River to produce hydroelectric power, which has reduced runoff from the former while increasing it in the latter (Stewart and Lockhart, 2004).

The effects of damming can be clearly seen in each of the four graphs in Figure 3.2. In all cases, the points of maximum and minimum discharge occur at roughly the same times in the cycle. However, for the dammed rivers, the maximums are not as high and the minimums not as low. For the period of May to November, the discharge from dammed rivers is lower than for undammed, and higher from December to April.

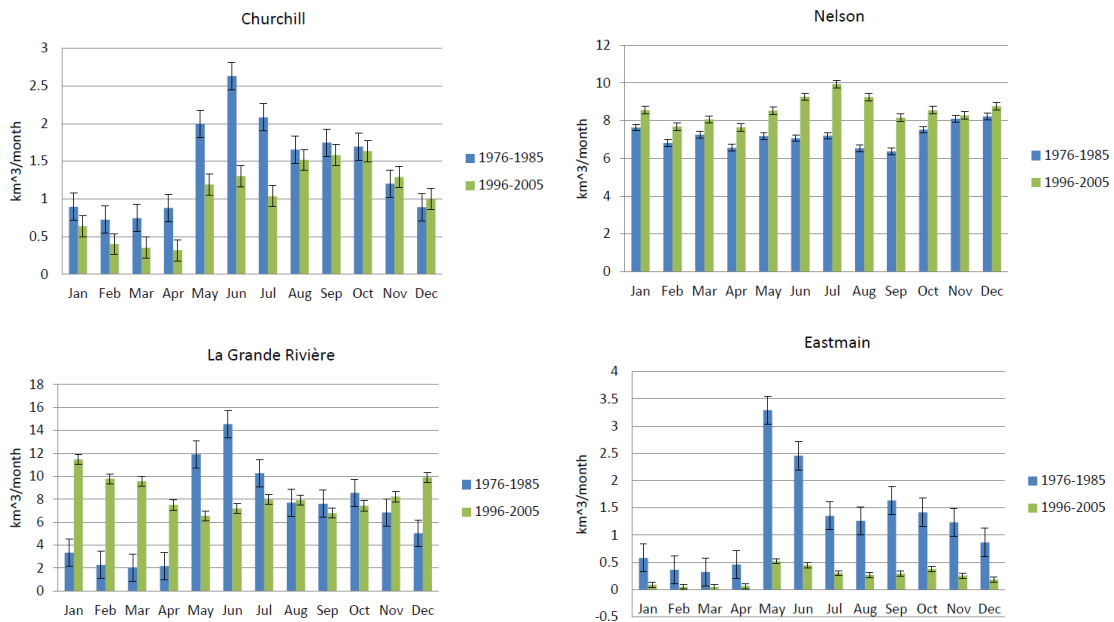


**Figure 3.2.** Comparison of runoff from four of the major rivers most affected by damming or diversion for the pre-1986 and post-1986 periods

### 3.2 Observed changes in river discharge to Hudson Bay

One important parameter which has the potential to impact the environment at the higher latitudes is the magnitude and seasonality of freshwater runoff into the polar seas. Variability in the water budget in such environmentally sensitive areas of the ocean affects salinity which in turn can affect such physical factors as sea ice formation and stratification of the water column. Climate models generally have proved to be sensitive to freshwater inflows (Hordoir et al., 2008). It is the modification or regulation of this volume of river runoff which is the subject of this thesis.

Figures 3.3 (a) and 3.4 (a) compare the discharge of all rivers for the pre-damming period (1964-1985) with the post-damming period (1986-2005). While the total annual discharge volume varies little from the earlier period to the later (a decrease from 528.0 km<sup>3</sup> to 513.3 km<sup>3</sup> or 4.7%), there is stronger evidence of a change in seasonality. The maximum monthly discharge for the pre-1986 period occurs in June, compared to a May maximum for the post-1986 period. Pre-1986, the total mean volume for the May-Nov period is 406.3 km<sup>3</sup> and 121.7 km<sup>3</sup> for Dec-Apr, compared to 373.0 km<sup>3</sup> and 137.4 km<sup>3</sup> respectively for post-1986.

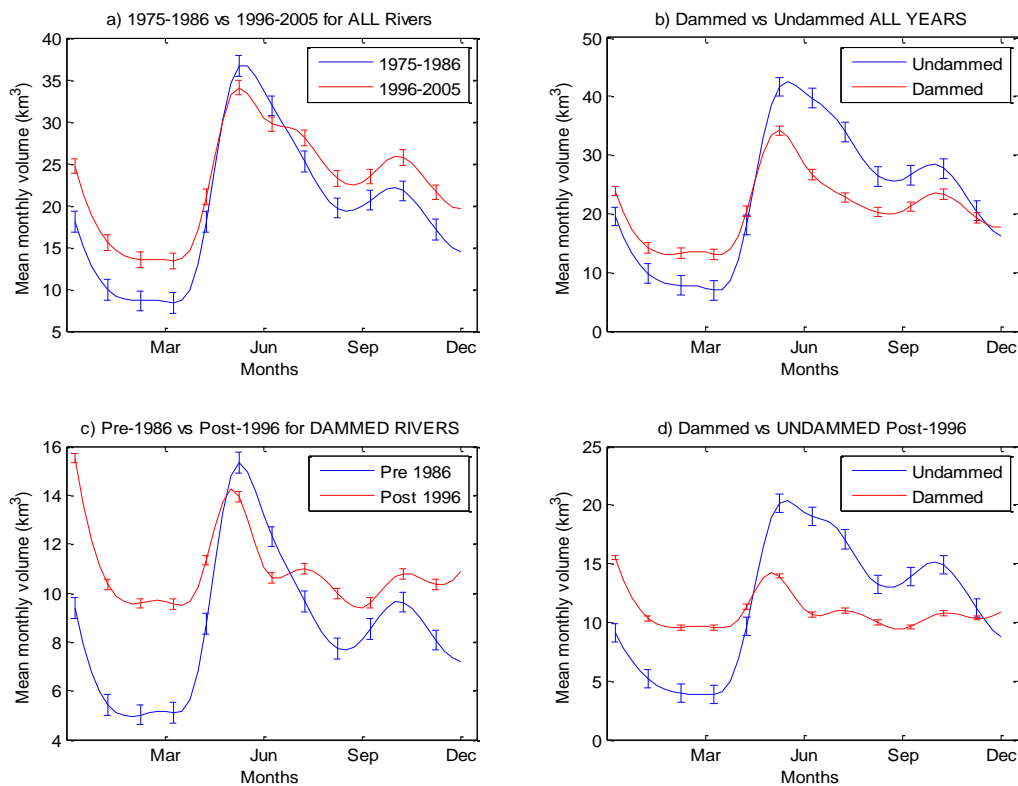


**Figure 3.3.** Monthly effects of damming on the volume of river runoff: a) Pre- vs Post damming for all rivers; b) Dammed vs Undammed for ALL Rivers; c) Pre – vs Post Damming for Dammed rivers; and d) Dammed vs Undammed for ALL Rivers, post-damming period.

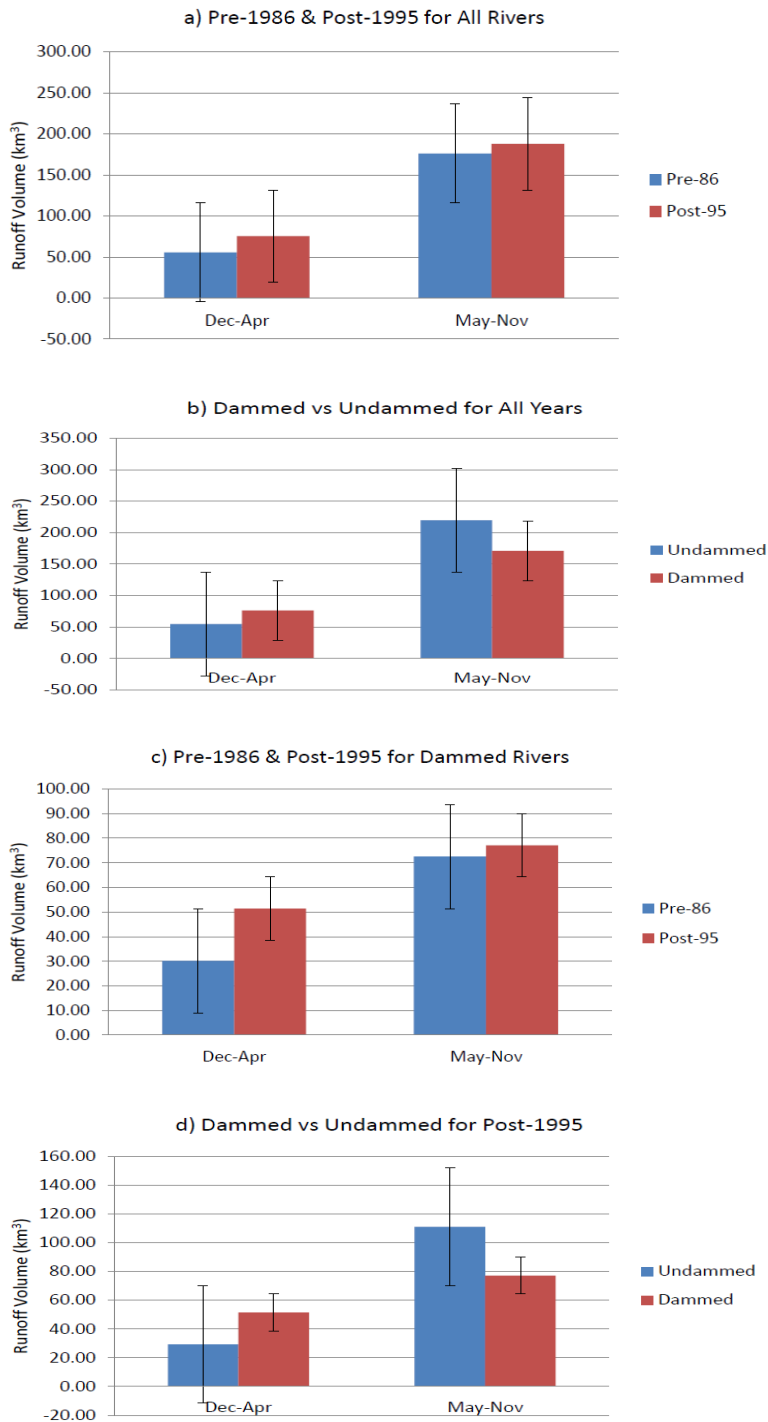


**Figure 3.4.** Seasonal effects of damming on the volume of river runoff

Figures 3.3 (d) and 3.4 (d) compare the discharge of undammed rivers to dammed rivers for the post-damming period (1986-2005). This comparison shows the most pronounced evidence of change in the seasonality of discharge. The maximum monthly discharge for the undammed rivers occurs in June, compared to a May maximum for the dammed rivers. For the undammed rivers, the total mean volume for the May-Nov period is 214.4 km<sup>3</sup> and 55.0 km<sup>3</sup> for the Dec-Apr period compared to 158.6 km<sup>3</sup> and 85.3 km<sup>3</sup> respectively for the dammed rivers.

## **CHAPTER 4. OCEANOGRAPHY OF HUDSON BAY – MODEL VERSUS OBSERVATIONS**

HBS an unusually fresh, large-scale arctic/subarctic estuarine system and the largest body of water in the world (area: about a million square kilometers) to completely freeze over in the winter and be ice-free in the late summer (Prinsenber, 1988). The ice cover and severe weather conditions makes it difficult to conduct continuous observations in the region. Observations are available for limited periods mostly during the summer and autumn seasons. In this chapter the results from model simulations are compared with existing observations.

The model and observations are largely in agreement in presenting very similar structures of the dynamics in Hudson Strait. Most importantly, the model correctly represents the near-shore, along-coastal currents and cross channel transport.

It should be noted that, while the data provides observations at the surface, the first model level is at 4 m depth. This discrepancy can cause differences between observations and model which cannot be accounted for here.

### **4.1 The Hudson Strait.**

The dynamics of Hudson Strait plays a key role of the exchange between Hudson Bay System and North Atlantic Ocean. The Drinkwater (1988) observational study revealed three distinctive features of the circulation through the Hudson Strait:

- 1) a southeastward current on the south side of the strait (out of the bay);

- 2) a northwestward current on the north side of the bay (towards Hudson Bay); and
- 3) a cross-channel flow at about the middle of the strait.

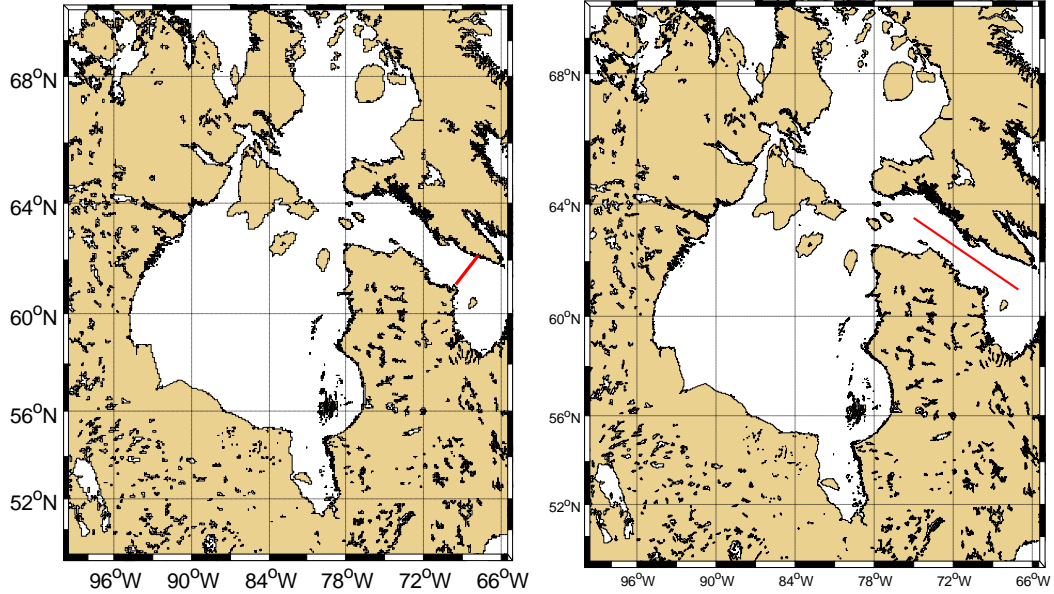


**Figure 4.1.** Locations of cross-channel (left) and along-channel transects of the study by Drinkwater (1988)

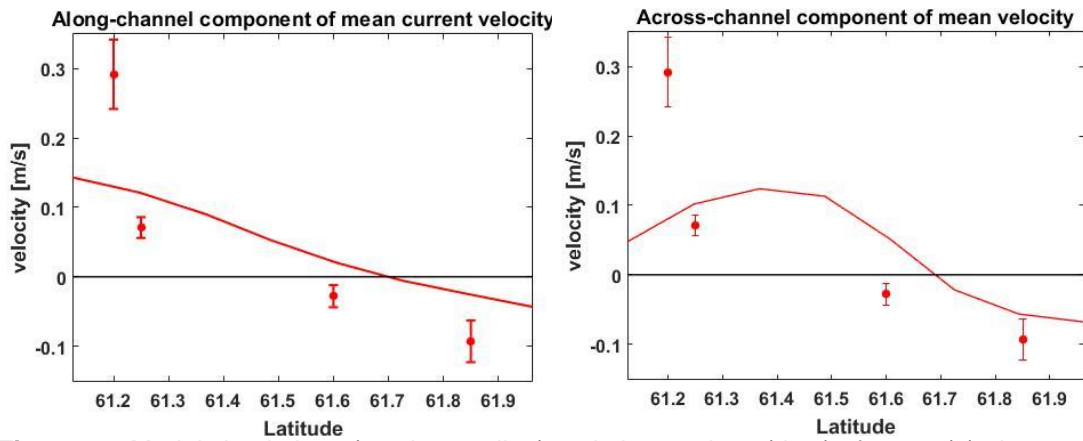


**Figure 4.2** Model simulations (continuous line) and observations (dots) of mean (a) along-channel and (b) across-channel velocity components.

Figure 4.2 shows the modeled versus observed along- and cross-channel component of surface current velocity. The along-channel velocity has a maximum

magnitude in the plume of surface fresh water exported out of the Hudson Strait along its southern coast. The observations suggest that the alongshore plume has a relatively small horizontal off-shore extension and velocity magnitude decreases towards the central part of the channel. The velocity along the northern coast of the Hudson Strait is directed inward from the Labrador Sea. This is the flow which brings salty and cold North Atlantic waters into the Hudson Bay System.

There is a cross-channel transport which according to the model and observations is directed towards the central part of the channel (Drinkwater, 1988). This is a dynamical factor that can potentially impact the mixing of the two water masses the fresh water with origin from Hudson Bay and salty Atlantic water flowing along the northern coast of the Hudson Strait. The simulated vertical structure of the flow averaged over the period from

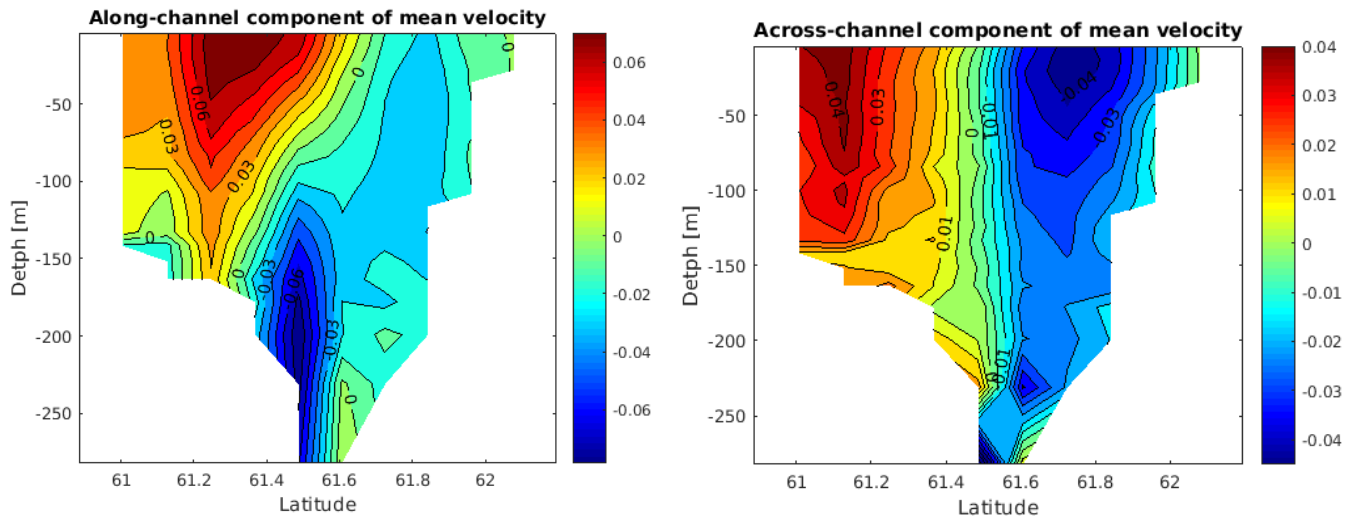


**Figure 4.3.** Simulated (a) along-channel and (b) cross-channel velocity components averaged over the period 1990-1999.

1990 to 1999 is shown on Figure 4.3. The southwestward plume along the southern coast of the Hudson Strait is a pattern which is well known from observational studies (see Straneo and Saucier, 2008). In particular, Straneo and Saucier (2008) found that the outflow from Hudson Strait has the typical characteristics of a buoyant coastal plume over sloping topography. The dynamics of this current is dominated by a balance between the frictional forces and the pressure gradient force due to the horizontal density gradients. The model results correspond well to the theoretical estimations of Straneo and Saucier (2008) who found that the plume spreads over the shelf slope and has extension about 25-30km in horizontal and depth of about 170m.

The model predicts a reverse of the direction of the current under the surface plume. Though no observations of currents at this depth exist, the data of Straneo and Saucier (2008) suggest that the current shows a strong rotation in the surface 100m layer. This rotation occurs on the northern edge of the plume. This is an area of large horizontal density gradient in the surface layer which, according to the thermal wind relation, drives a rotation in the direction of current velocity with depth. The flow in the northern part of the Hudson Strait is weaker and directed westward in the whole water column representing the transport of Baffin Bay and Labrador Sea waters into the Hudson Bay system.

The cross-channel flow is surface intensified and has direction towards the center of the Hudson Strait. Drinkwater (1988) observed this flow convergence in the surface layer only. His results for the cross-channel velocity in the subsurface layer were not

conclusive. The reason for this is that as the model results and Drinkwater (1988) observations suggest that the cross-channel velocity has a relatively small magnitude of 1 cm/s. This velocity convergence in the Hudson Strait is factor that may contribute to the mixing of river plume and Baffin Bay. While this mixing happens in the Hudson Strait, its mechanism remains not well understood (see Straneo and Saucier, 2008).

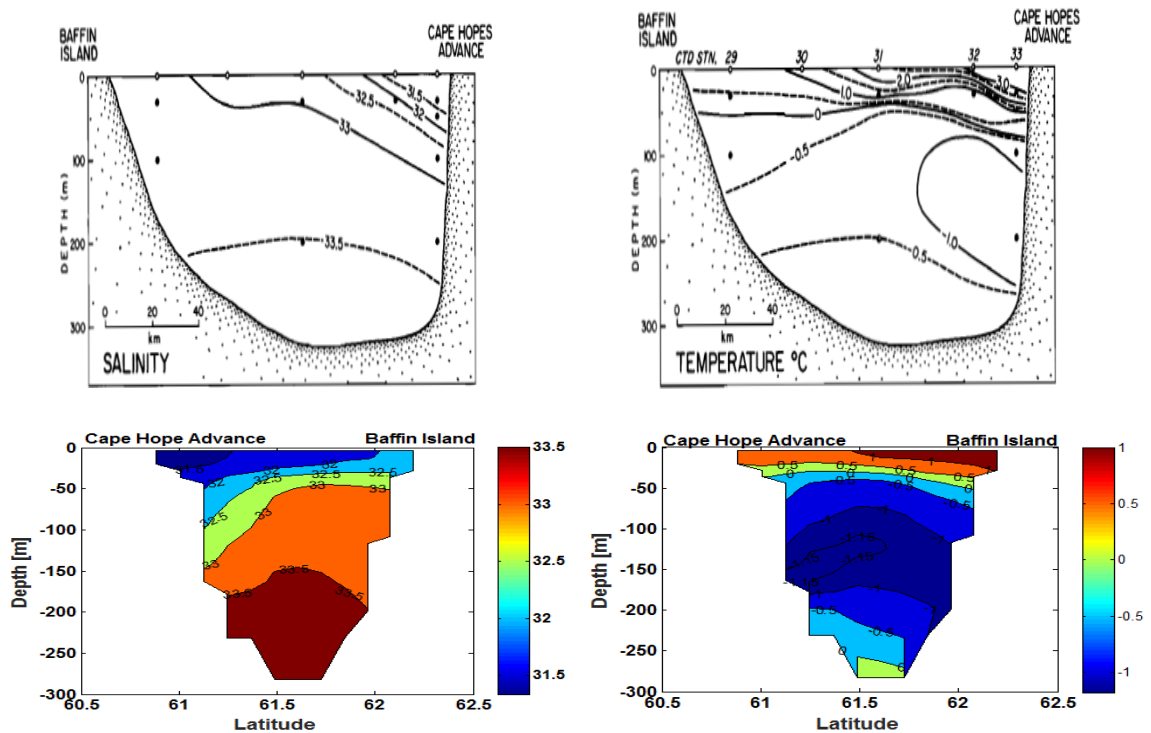


**Figure 4.4** Observed cross-channel salinity and temperature (upper panels) and simulated salinity and temperature (bottom panels)

Model simulations closely resemble the observed temperature and salinity across the channel (Figure 4.4). The salinity has a minimum of about 31.5 in the along shore plume originating from Hudson Bay. The salinity of the Baffin Bay waters which enter along the northern coast of the strait is about 32.5 psu in both model and observations. The bottom layer salinity is close to 33.5 psu. Comparison with the Figure 4.3 suggest

that area with salinity higher than 33 psu coincides approximately with the area where the along channel velocity is negative, i.e. this is the area of inflow of Atlantic waters. The area of counter current (Figure 4.3) at depths between 150 and 200m coincides with the area of temperature minimum.

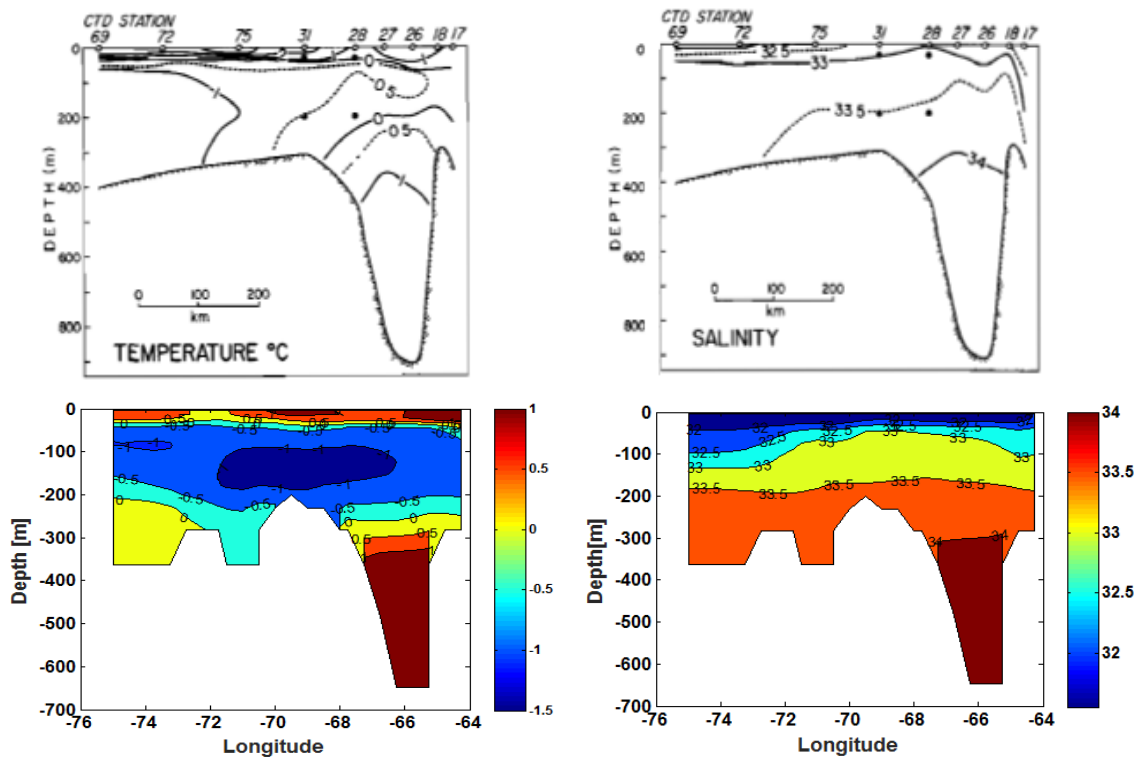
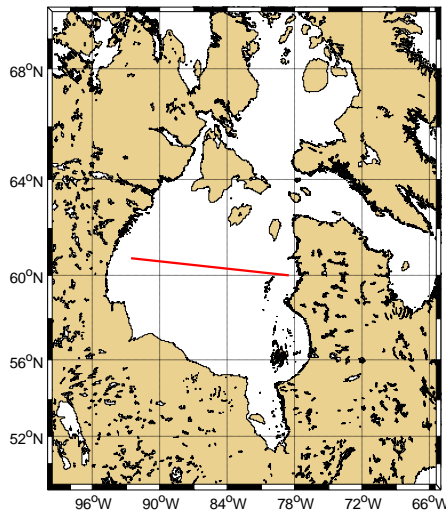


**Figure 4.5.** Observed (upper panel) and simulated (bottom panel) along-channel temperature and salinity

Figure 4.5 shows a westward penetration of cold and salty waters from the Labrador Sea at depths between 100 and 200m. The fresh surface waters from Hudson Bay occupy approximately the surface 50m layer. The cold and salty intermediate waters lay underneath the surface layer. Drinkwater (1988) data and our simulations suggest that these waters extend along channel in the eastern end of the Hudson Strait.

## 4.2 Hudson Bay

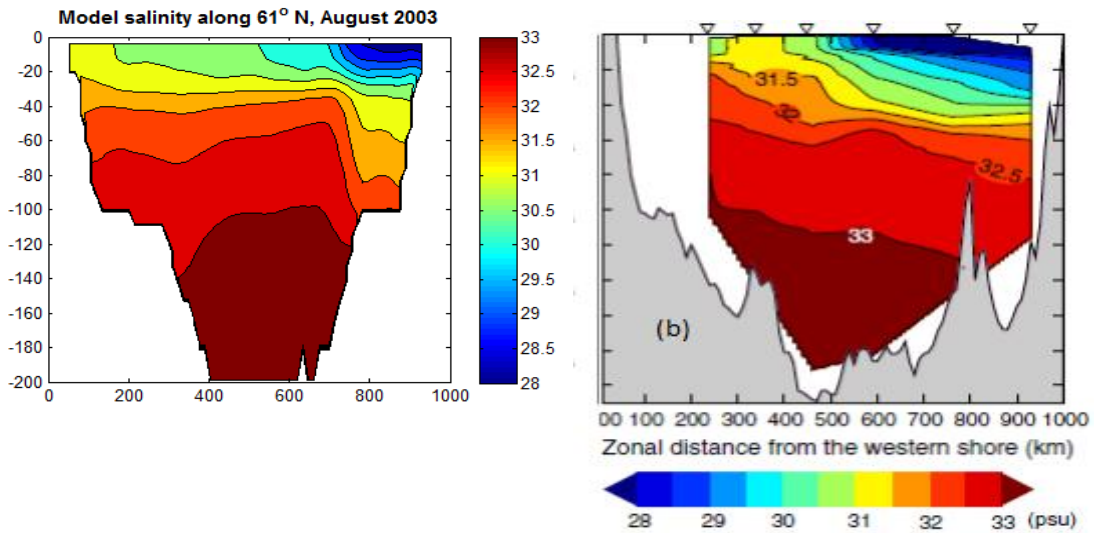
Several data sets were used to validate our model in Hudson Bay: observations by St. Laurent et al., 2011, observations by Lapoussière et al. (2009), Saucier et al. (2004), and data from the Canadian Ice Service for 1997. The study by St-Laurent (2011) produced a salinity profile along the transect shown in figure 4.6.



**Figure 4.6.** Location of the salinity profile from St-Laurent et al. (2011)

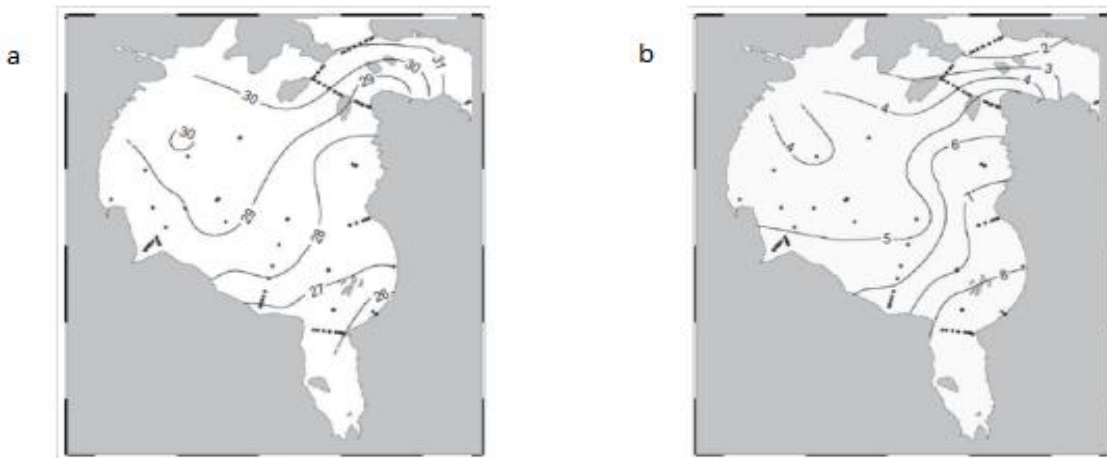
The observed salinity profile produced by the St. Laurent et. al. study and the salinity profile along the same transect from our model in this study is shown in Figure 4.7. The model represents correctly the presence of layer with salinity of 33psu. This is salinity higher than the salinity of all water masses entering Hudson Bay. Its presence is explained by previous studies with the role of the brine release during freezing of surface layer and vertical convection driven by the increased salinity and cooling of the surface layer. In the model solution the river plume of low salinity in the surface layer in the

eastern part of the basin is bounded by the rim current. In the model solution this current is associated with high horizontal salinity gradients at about 700km.



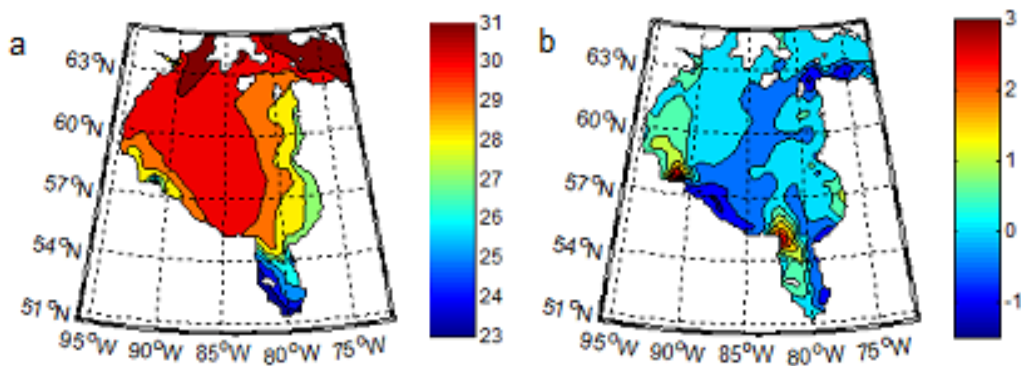
**Figure 4.7.** Salinity along 61°N in August 2003 according to (a) model simulation and (b) observations (St. Laurent et al., 2011). Contour interval of the both figures is 0.5 psu.

Figure 4.8 shows a comparison of model results with observations by Lapoussière et al. (2009). Figures 4.8 (a) and (b) show observed sea-surface salinity and temperature based on those observations, while Figures 4.9 and 4.10 show plots of the corresponding data from the model results.



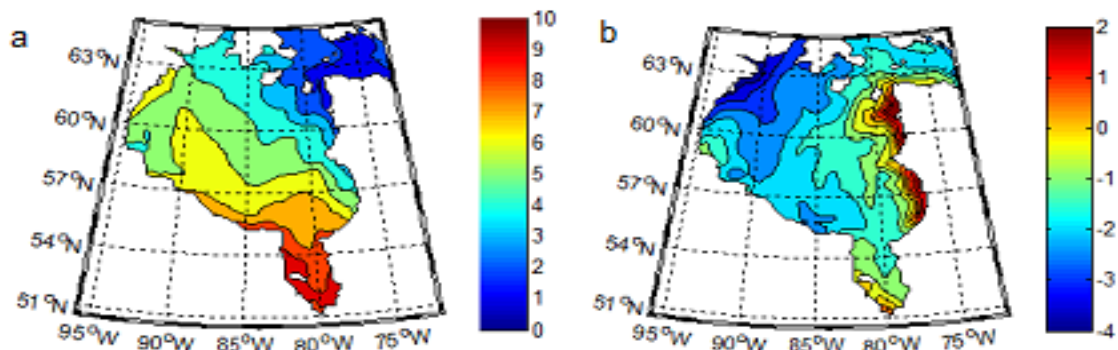
**Figure 4.8.** Sea surface (a) salinity and (b) temperature from observations (Lapoussière et al., 2009)

Figure 4.8 shows the observations of surface temperature and salinity made by Lapoussière et al. (2009) in the Autumn of 2005. The position of observational stations are shown as dots. The river plume in the eastern part is a surface water mass of low salinity and high temperature. The off-shore extension of the plume not well resolved by these observations (see for instance Figure 1.11). The salinity in the northwestern part represent the relatively salty (30psu) and cold (4°C) of Arctic origin.



**Figure 4.9.** Simulated (a) surface salinity (psu) and (b) salinity tendency (psu/month) for September – October, 2005.

Model simulations for post-damming period with actual river runoff overestimate salinity in the northwestern part of the basin by about 1 psu. This is the value by which the salinity of simulated Arctic waters exceed the observed salinity in this part. There are no observational station in this part of the basin which suggest that much of the contours there on Figure 4.8a are result from extrapolation and conclusions about the model – observations differences is difficult to make. The simulated salinity in the central part of Hudson Bay, however, is also higher than the observed one by about 1-2 psu. This difference between model and data can be caused by uncertainties in the surface precipitation minus evaporation. One factor which can contribute to this difference is also the fact that the observations are done over a period of four weeks at the September and beginning of October. The ocean is intensively cooled during this period and the surface layer mixes with the subsurface waters. One characteristic of the effect of the temporal variability is the salinity tendency (psu/month) calculated based on the model solution (Figure 4.9b). It defines the rate of the change of the surface salinity during the period of the observations.



**Figure 4.10.** Simulated (a) sea surface temperature and (b) tendency of sea surface temperature (°C/month)

In the same way, the simulated (Figure 4.10a) and observed (Figure 4.8b) have many common elements. The shallow waters of James Bay have temperatures between 8 and 9 degrees while waters in the northwestern part of the basin have temperatures down to 4 degrees. Again there is strong temporal change in temperature during the period of observations. In the northwest part it cools at rate 1 degree/month and in the eastern part it warms at 2 degrees/month.

Both model and observations show a presence of relatively warm and fresh surface plume which spreads along the east coast of Hudson Bay. Salty and cold surface Arctic waters enter the basin from northwest and flow into the central part of the basin. The shallow James Bay is the part of the basin which is strongly influenced by the river inflow. Its salinity is below 26 psu and temperature around 9 to 10 degrees.

Figure 4.11 shows Canadian Ice Service observations and model results for the concentration and ice thickness during the in winter of 1996-1997. In the beginning of winter, the ice forms first in the northern and north-west part of Hudson Bay.

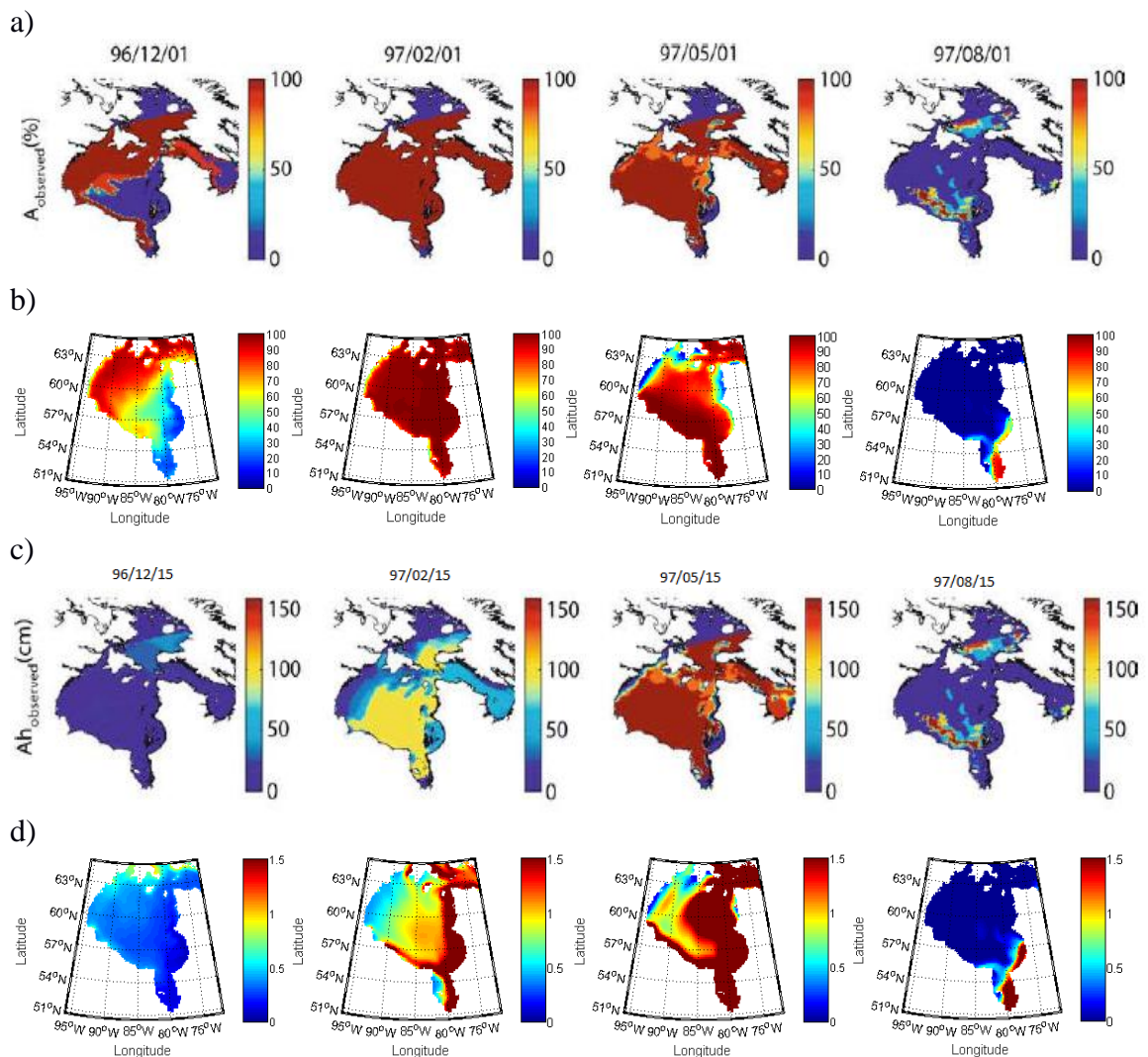


**Figure 4.11.** Comparison of model simulation with sea-ice charts from the Canadian Ice Service for the period of Dec 1996 – August 1997. The first two rows are (a) observed and (b) modeled sea-ice concentration in (%); the last third and fourth rows are (c) observed and (d) modeled sea-ice thickness in cm (0-150) and metres (0-1.5). Note that the data is not available for southern James Bay and are shown as zero values in the observation graphs.

The thickness is less than 0.5 m in the whole basin. In February, Hudson Bay is completely covered by ice. The thickness varies from about 50cm in the eastern to about 2.00 m in near the western coast of the basin. The pattern of thickness of sea-ice in the

western part coincides with the area of the river plume and low surface salinity. The winter air temperature in this part is not colder than over the rest of Hudson Basin. One possible factor that eventually triggers the larger sea-ice production is the eastern part is the low surface salinity. Freezing temperature decreases with increase of salinity, and therefore freshwaters in the eastern part freeze easier. Another factor that potentially can influence the sea-ice dynamics is the circulation and wind stress. According to model and data, in the spring sea-ice starts to melt first in the northern and north-western part of the basin. In the summer some sea-ice is still remaining in the southeastern part of Hudson Bay.

## **CHAPTER 5. IMPACT OF RIVER RUNOFF CHANGES**

This study is focused on the impact of river run-off on the oceanographic characteristics of Hudson Bay. Some earlier studies were based on the assumption that the flow of river runoff through the system to be analogous to a “pipeline” or channel of fresh water from the river sources through the Hudson Strait to the Labrador Sea. Although studies from Meyers et al. (1990) and Déry et al. (2005) differed in their estimate of the transit time for the waters to reach the Labrador Sea (nine months and three years respectively), both assume the water to be advected as in a pipeline where the outflow downstream is determined strictly by the freshwater input upstream. More recent studies demonstrate that this is not the case within Hudson Bay because the waters are redistributed between the near shore outflow from the rivers and the interior of the bay (St-Laurent et al., 2011). Here we use the results from the two model experiments to identify how the changes of river run-off because of the hydropower production affected the redistribution of the freshwaters inside the basin.

The analysis presented in Chapter 3 demonstrates that two types of changes occurred in the river discharge since the mid-1970s. Firstly, the annual cycle in some of the rivers input flattened because of intensified winter river flow. Secondly, some of the rivers were diverted, so the river runoff in these areas decreased since the 1970s.

Figure 5.1 shows the location of the major rivers which were affected by damming and diversions. The majority of the river runoff changes occurred in the southern part of the system in the James Bay.

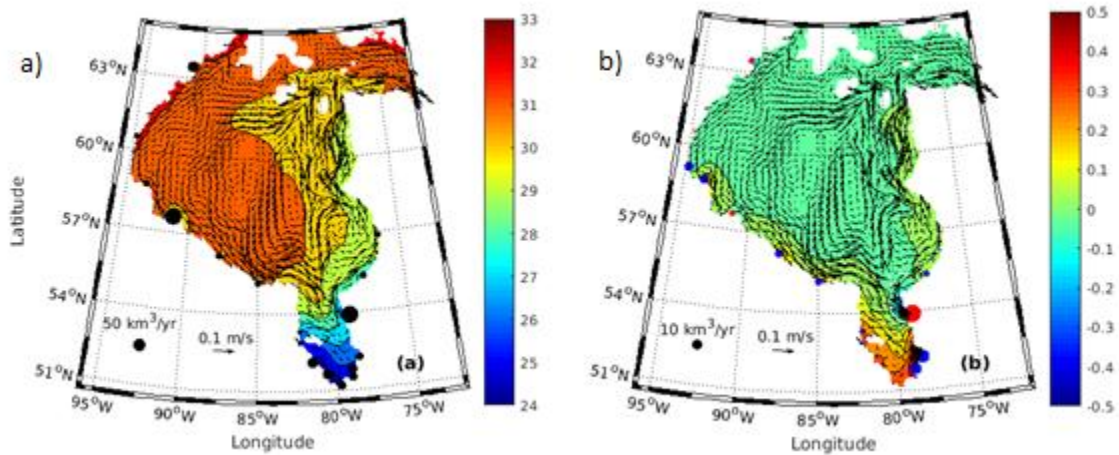


**Figure 5.1.** Annual mean river flow with averaged SSS (a) and river flow change with salinity difference (b). The location and relative flow of the major rivers are indicated and the change in flow shown as positive (red) or negative (blue) and model surface circulation is indicated by the vector plot.

Figure 5.1a shows the position of the major rivers entering Hudson Bay. The lowest salinity is observed in the region (see also observations on Figure 1.10) of the southern James Bay. There are a number of rivers in this region which were diverted into the La Grande River. The river runoff from the La Grande contributes to the formation of freshwater along the east coast. This surface water mass, however, mixes (Fig 5.1a) with the surrounding waters (see also St-Laurent et al., 2011). Because of this strong mixing, the effect of the increase in the freshwater discharge (Fig. 5.1a) on the salinity anomaly is relatively weak and hardly seen in the model solution.

A number of rivers in the southern part of the James Bay were diverted into the La Grande River. This caused a reduction of the annual mean river discharge and as a result – a positive salinity anomaly in this region. Unlike the offshore regions of discharge of the La Grande River and Nelson river, the currents inside the James Bay are relatively weak and the positive salinity anomaly remains persistent in the James Bay.

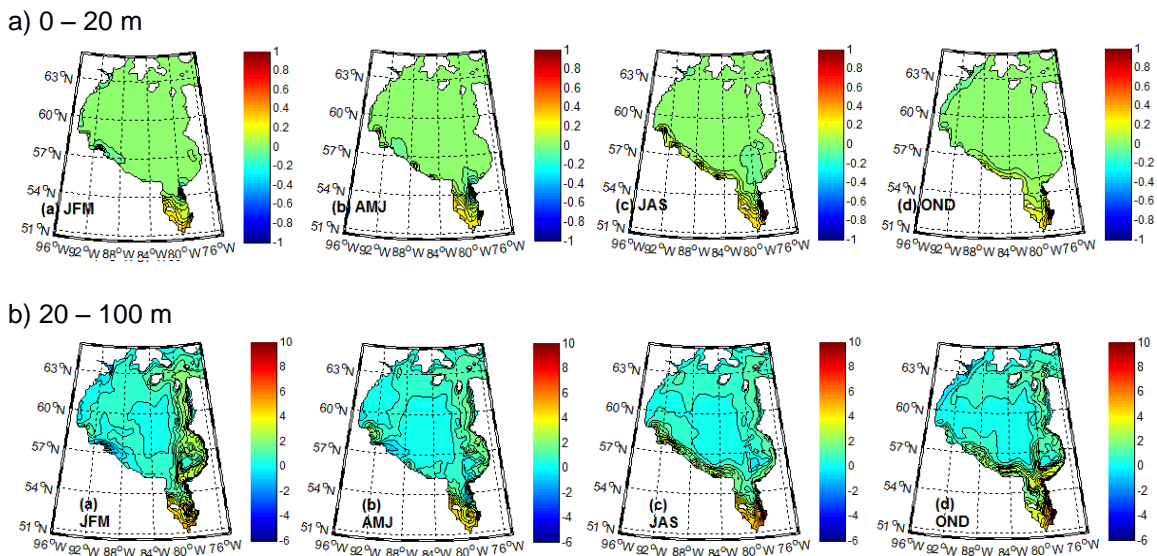


**Figure 5.2.** Seasonally averaged difference of salinity at 0-20 m (a) and salinity content ( $\text{kg/m}^2$ ) in the 20-200m. The averaging periods are, left to right: Jan-Feb-Mar, Apr-May-Jun, Jul-Aug-Sep, and Oct-Nov-Dec.

Figure 5.2 shows the salinity, seasonally averaged over the study period, at 0 – 20 m and the salinity content ( $\text{kg/m}^2$ ) at 20 – 200 m. The increased surface salinity reduces the hydrostatic stability of the water column. The intensified vertical mixing propagates the surface salinity anomaly deeper into the waters of the James Bay.

## CHAPTER 6. CONCLUSIONS

The impact of hydropower development on the oceanography of Hudson Bay is studied through a simulation experiment using the *Nucleus for European Modelling of the Oceans* (NEMO) ocean model. The total study period was from 1964 – 2005, and two experiments were run corresponding to the periods before and after 1986 which is when the major hydropower developments were completed. The two model experiments were run using different river runoff data as follows:

1. Actual river runoff for the whole study period 1964 to 2005
2. Actual river runoff from 1964 – 1985 and monthly mean runoff based on pre-86 data for the period 1986 – 2005.

The second experiment was used to simulate what would have happened if the hydropower developments had not occurred.

Two major changes in the river discharge are found since the mid-1970s when the major hydropower developments began

- reduction in the seasonal cycle of river input in some of the station
- change in the positions of the major river inputs because of the river diversion

The main impact of this development was found in James Bay where the salinity of the surface layer increased by about 0.2-0.3 psu. This positive salinity “anomaly” was caused by the diversion of some major rivers from southern James Bay, an area of relatively low coastal circulation, to northern James Bay, near the mouth of the bay where circulation

and transport is much higher. This resulted in more freshwater being advected away, leaving behind water with higher salt content.

This salinity “anomaly” intensifies in the summer season when it affects also the salt content below the thermocline. In the following autumn and winter season the salinity anomaly is traced along the main current up to the Hudson Strait

## **CHAPTER 7. FUTURE WORK**

Observations in Hudson Bay are limited because of the severe weather conditions. More observations, specifically in James Bay, are needed to increase the concentration of available data in time and space. A more thorough data set will help better understand how the region is influenced by the river diversion projects.

As well, further model studies of the effect of high frequency processes such as tides, coastal density plumes and currents are needed to better understand the response of Hudson Bay on the long term changes in river run-off.

We found that James Bay and the area of alongcoastal river plume are the regions most sensitive to variations in the river discharge. These also the regions wher most significant environmental change can be expected in response to hydroelectric development projects. Future observations in this area will be highly valuable for estimating the environmental impact of river discharge variations. More observations are needed also about sea ice thickness in the coastal areas.

The second characteristic which is important for the dynamics of Hudson Bay is the sea ice. More observations are needed about sea ice thickness in the coastal areas.

The Hudson Strait is the region which is crucially important for the dynamics of the Hudson Bay System. Very few observations are available for its eastern part and its opening to the Labrador Sea. No observations are available in the central and western parts of the strait. New observations in this part of the Hudson Bay system are needed in order to understand the dynamics of the Arctic – North Atlantic exchange.

## References

- Danielson, EW Jr., 1969. The surface heat budget of Hudson Bay. Marine Sci MS Report, 9, McGill University, Montreal, Canada pp 196
- Déry SJ, Mlynowski TJ, Hernández-Henríquez MA, Straneo F, 2011. Interannual variability and interdecadal trends in Hudson Bay streamflow. *Journal of Marine Systems* 88, 341–351
- Déry, SJ, Stieglitz, M, McKenna, EC, Wood, EF, 2005. Characteristics and trends of river discharge into Hudson, James, and Ungava Bays, 1964 – 2000. *J. Climatol.* 18, pp 2540 –2557
- Déry SJ and Wood EF, 2004. Teleconnection between the Arctic Oscillation and Hudson Bay river discharge. *Geophysical Research Letters*, 31
- Dickson B, Meincke J, Rhines P, 2008. Arctic-subarctic ocean fluxes: defining the role of oceans fluxes in climate, pp 1-13
- Drinkwater KF, 1986. Physical oceanography of Hudson Strait and Ungava Bay. In Martini EP (ed) *Canadian Inland Seas*, Oceanogr Ser 44 Elsevier New York, pp 237–261
- Drinkwater KF, 1988. On the Mean and Tidal Currents in Hudson Strait. *Atmosphere-Ocean* 26, pp 253–266
- Drinkwater KF, Taylor GB, Petrie, WB, 1991. Temperature, salinity, and density data from the Hudson Strait Region during August–September, 1982. *Can Data Rep Hydrogr Ocean Sci*, pp 99
- Freeman NG, Murty TS, 1976. Numerical modelling of tides in Hudson Bay. *J Fish Res Board Can* 33, pp 2345–2361
- Gaston, AJ and Hipfner, JM, 1998. The effect of ice conditions in northern Hudson Bay on breeding by thick-billed murres (*Uria lomvia*). *Canadian Journal of Zoology*, 76, pp 480 – 492
- Gent, PR, McWilliams, JC, 1990. Isopycnal mixing in ocean circulation models. *J. Phys. Oceanogr.* 20, pp 150–155

- Granskog, M.A., Macdonald, R.W., Kuzyk, Z.A., Senneville, S., Mundy, C.J., Barber, D.G., Stern, G.A., Saucier, F.J., 2009. Coastal conduit in southwestern Hudson Bay (Canada) in summer: rapid transit of freshwater and significant loss of colored dissolved organic matter. *J. Geophys. Res.*, p 114
- Ingram RG, Prinsenberg SJ, 1998. Coastal oceanography of Hudson Bay and surrounding eastern Canadian Arctic waters. In: Robinson AR, Brink KH (eds) *the sea*, vol. 11 - the global coastal ocean, regional studies and syntheses, Chichester UK Wiley, pp 835–861
- Jones EP, Anderson LG, 1994. Northern Hudson Bay and Foxe Basin: water masses, circulation and productivity. *Atmos Ocean* 32, pp 361–374
- Lapoussière, A, Michel, C, Gosselin, M, Poulin, M, 2009. Spatial variability in organic material sinking export in the Hudson Bay system, Canada, during fall. *Cont. Shelf Res.* 29, pp 1276–1288.
- LeBlond, PH, TR Osborn, DO Hodgins, R Goodman, and M Metge, 1981. Surface circulation in the western Labrador Sea. *Deep Sea Res.* 28A
- Lentz, SJ, 2004. The response of buoyant coastal plumes to upwelling-favorable winds. *J. Phys. Oceanogr.* 34, pp 2458–2469
- Madec, Gurvan, 2008. NEMO ocean engine, France Institut Pierre-Simon Laplace (IPSL) 300pp. (Note du Pole de Modélisation, 27)
- Manak, DK and Mysak LA, 1989. On the relationship between Arctic sea-ice anomalies and fluctuations in northern Canadian air temperature and river discharge. *Atmos-Ocean* 27:4, pp 682-691
- Marshall, IB and PH Schut, 1999. A national ecological framework for Canada: overview. Environment Canada, Ecosystems Science Directorate and Agriculture and Agri-Food Canada, Research Branch, Ottawa.
- Maxwell, IB, 1986: A Climate Overview of the Canadian Inland Seas. In *Canadian Inland Seas*, Elsevier Oceanography Series, 44, pp 79-99.
- Mertz G, Narayanan S, Helbig J., 1993. The freshwater transport of the Labrador Current. *Atmos-Ocean* 31, pp 281–295

- Messier, D, RG Ingram, and D Roy, 1986. Physical and biological modifications in response to La Grande hydroelectric complex. p. 403-424. In I.P. Martini (ed.) Canadian Inland Seas. Pp 494
- Milko R, 1986. Potential ecological effects of the proposed Grand Canal Diversion project on Hudson and James bays. ARCT 39(4), pp 316–326
- Myers, R.A., Akenhead, S.A., Drinkwater, K., 1990. The influence of Hudson Bay runoff and ice-melt on the salinity of the inner Newfoundland Shelf. Atmos. Ocean 28, pp 241–256
- Prinsenber SJ, 1983. Effects of the hydroelectric developments on the oceanographic surface parameters of Hudson Bay. Atmos-Ocean 21, pp 418–430
- Prinsenber SJ, 1986a. Salinity and temperature distribution of Hudson Bay and James Bay. In: Martini EP (ed) Canadian Inland Seas, Oceanogr Ser 44, Elsevier, New York, pp 163–186
- Prinsenber SJ, 1986b. The circulation pattern and current structure of Hudson. In: Martini EP (ed) Canadian Inland Seas, Oceanogr Ser 44, Elsevier, New York, pp187–203
- Prinsenber SJ, 1986c. On the physical oceanography of Foxe Basin. In: Martini EP (ed) Canadian Inland Seas, Oceanogr Ser 44, Elsevier, New York, pp 217–236
- Prinsenber SJ, 1988. Ice-cover and ice-ridge contributions to the freshwater contents of Hudson Bay and Foxe Basin. ARCT 41(1), pp 6–11
- Prinsenber SJ, 1991. Effects of hydro-electric projects on Hudson Bay's marine and ice environments. James Bay Publication Series No. 2
- Prinsenber SJ, Freeman NG, 1986. Tidal heights and currents in Hudson Bay and James Bay. In: Martini EP (ed) Canadian Inland Seas, Oceanogr Ser 44, Elsevier, New York, pp 205–216
- Prinsenber SJ, Loucks RH, Smith RE, Trites RW, 1987. Hudson Bay and Ungava Bay runoff cycles for the period 1963–1983. Can Tech Rep Hydro Ocean Sci, pp 92 71

- Prinsenber, SJ and Weaver, RK, Hudson Bay oceanographic data report, 1982. Canada Department of Fisheries and Oceans, Ocean Sciences and Surveys, Bayfield Laboratory for Marine Science and Surveys, Burlington, ON. Data Report Series No. 1983; 83-5:vii p 221
- Sadler HE, 1982. Water flow into Foxe basin through Fury and Hecla Strait. *Naturaliste Can* 109, pp 701–707
- Saucier, F.J., Senneville, S., Prinsenber, S., Roy, F., Smith, G., Gachon, P., Caya, D., Laprise, R., 2004. Modelling the sea ice-ocean seasonal cycle in Hudson Bay and Hudson Strait, Canada. *Climate Dynamics* 23, pp 303-326.
- Stewart, RH, 1997. Introduction to Physical Oceanography. Texas A&M University, p 51
- Stewart, D.B., and W.L. Lockhart, 2004. Summary of the Hudson Bay Marine Ecosystem Overview. Canadian Department of Fisheries and Oceans
- St-Laurent, P., Straneo, F., Dumais, J.-F., Barber, DG, 2011. What is the fate of the river waters of Hudson Bay? *J Marine Systems* 88, pp 352-361.
- Straneo, F., Saucier, FJ, 2008. The outflow from Hudson Strait and its contribution to the Labrador Current. *Deep Sea Res. I* 55 (8), 926 - 946.
- Thorndike AS, Rothrock DA, Maykut GS, Colony R, 1975. The thickness distribution of sea ice. *J Geophys Res* 80, pp 4501–4513
- Van Loon, H. and R.A. Madden. 1981. The South Oscillation. Part 1: Global associations with pressure and temperature in northern winter. *Mon. Weather Rev.* 109, pp 1150-1162
- Wang J, Mysak L, Ingram RG, 1994a. A numerical simulation of sea ice cover in Hudson Bay. *J Phys Oceanogr* 24, pp 2515–2533
- Wang J, Mysak L, Ingram RG, 1994b. Interannual variability of sea-ice cover in Hudson Bay, Baffin Bay and the Labrador sea. *Atmos-Ocean* 32, pp 421–447